



# **Interdisciplinary Scientific and Technical Research for SDG Achievement**

**December 2025**

**Dr. M. KOTTEESWARAN**

**Associate Professor, Department of MBA  
Vels Institute of Science, Technology & Advanced Studies  
(VISTAS), Chennai, India.**

**Dr. J. SATHIYA SAVITHRI**

**Head and Assistant Professor  
PG and Research Department of Chemistry  
Theivanai Ammal College for Women (Autonomous)  
Villupuram, India**

**Dr. ABSARA FDO S**

**Assistant Professor, Department of Chemistry  
Vels Institute of Science, Technology & Advanced Studies  
(VISTAS), Chennai, India.**

**Dr. M. RAMAMURTHY**

**Assistant Professor, Department of Marine Engineering  
Academy of Maritime Education and Training (AMET)  
Deemed to be University, Kanathur, Chennai, India.**

December 2025

ISBN: 978-81-993402-8-2



© Copyrights reserved by Authors and Publishers

*Despite our best efforts, there is still a risk that some errors and omissions might occur unintentionally.*

*Without the prior consent of the authors and publishers, no part of this publication may be duplicated in any form or by any means, whether electronically, by photocopying, or otherwise.*

*The opinions and findings expressed in the individual chapters are those of the authors and the book's editors, not the publishers.*

*Cover page images attributed from [www.freepik.com](http://www.freepik.com), [www.vecteezy.com](http://www.vecteezy.com)*

Published By



**SCIENTIFIC RESEARCH REPORTS**  
(A Book Publisher, approved by Govt. of India)

I Floor, S S Nagar, Chennai - 600 087,  
Tamil Nadu, India.

[editors@srrbooks.in](mailto:editors@srrbooks.in), [contact@srrbooks.in](mailto:contact@srrbooks.in)  
[www.srrbooks.in](http://www.srrbooks.in)

## PREFACE

Achieving the Sustainable Development Goals (SDGs) requires a fundamental shift in how scientific inquiry and technological innovation are conceived, executed, and translated into practice. Complex global challenges such as climate change, resource scarcity, pollution, and sustainable industrialization cannot be addressed within the boundaries of a single discipline. Instead, they demand interdisciplinary scientific and technical research that integrates materials science, engineering, environmental science, energy systems, and industrial technologies. This book **“Interdisciplinary Scientific and Technical Research for SDG Achievement”** is grounded in the belief that collaborative, cross-disciplinary approaches are essential for developing practical solutions that align technological advancement with sustainability imperatives.

A central focus of contemporary sustainability research is the transition from linear production models to circular manufacturing systems. The development and application of sustainable natural fiber technologies illustrate how renewable resources can be engineered to replace conventional, resource-intensive materials. By embedding circularity into material design and processing, these approaches reduce environmental footprints while creating new value chains that support rural economies and responsible consumption patterns.

Advances in nanomaterials and smart surface technologies further demonstrate the role of cutting-edge science in enabling greener mobility systems. Through enhanced durability, reduced friction,

improved corrosion resistance, and multifunctional performance, these innovations contribute to energy efficiency and emissions reduction in transportation and infrastructure. Such solutions highlight how nanoscale engineering can deliver macroscopic sustainability benefits.

Urban sustainability is increasingly dependent on the ability to transform waste streams into valuable resources. Advanced conversion technologies, supported by chemical, thermal, and biological processes, offer pathways to reduce landfill dependency while recovering energy, materials, and nutrients. These systems not only address waste management challenges but also support resilient urban ecosystems and circular resource flows.

The integration of renewable energy into automated and digitally controlled industrial processes represents another critical dimension of sustainable development. Intelligent energy management, coupled with renewable generation, enhances operational efficiency, reduces carbon intensity, and supports flexible, low-emission manufacturing environments. This integration underscores the importance of aligning energy transitions with industrial automation.

Finally, the development of biodegradable composite materials reflects the growing emphasis on eco-friendly engineering solutions that balance performance with environmental responsibility. By combining material innovation with lifecycle thinking, such research contributes to sustainable product development across diverse applications. Collectively, the themes explored in this volume emphasize the pivotal role of interdisciplinary research in advancing

the SDGs, offering scientifically rigorous and technologically viable pathways toward a more sustainable and equitable future.

We extend our sincere thanks to our publisher, **Scientific Research Reports, Chennai, India**, for their dedicated efforts in preparing this book and for ensuring the inclusion of enriched and high-quality technical content.

*Wishes and Regards,*

**Dr. M. KOTTEESWARAN**

Department of MBA

Vels Institute of Science, Technology & Advanced Studies (VISTAS)  
Chennai, India.

**Dr. J. SATHIYA SAVITHRI**

PG and Research Department of Chemistry

Theivanai Ammal College for Women (Autonomous)  
Villupuram, India

**Dr. ABSARA FDO S**

Department of Chemistry

Vels Institute of Science, Technology & Advanced Studies (VISTAS)  
Chennai, India.

**Dr. M. RAMAMURTHY**

Department of Marine Engineering

Academy of Maritime Education and Training (AMET)  
Deemed to be University, Kanathur, Chennai, India.

# CONTENTS

Section No	Section Titles	Page No
1	Sustainable Natural Fiber Technologies for Circular Manufacturing	1-22
2	Nanomaterials and Smart Coatings for Green Mobility Solutions	23-45
3	Advanced Waste-to-Resource Conversion Technologies for Urban Sustainability	46-74
4	Renewable Energy Integration in Automated Industrial Processes	75-98
5	Biodegradable Composite Materials for Eco-Friendly Engineering Applications	99-127



## Section 1

# Sustainable Natural Fiber Technologies for Circular Manufacturing

### 1.1 Introduction

Natural fiber engineering represents a transformative approach to sustainable manufacturing, offering viable alternatives to synthetic, petroleum-based materials that dominate contemporary industrial production. The transition toward **bio-based fiber systems** addresses critical environmental challenges including resource depletion, carbon emissions, and accumulating non-biodegradable waste in terrestrial and marine ecosystems. Natural fibers derived from plants such as flax, hemp, jute, kenaf, bamboo, and sisal provide renewable material streams that can be cultivated, processed, and reintegrated into biological or technical cycles with minimal environmental impact (Faruk et al., 2012). These materials demonstrate mechanical properties comparable to glass fibers in specific applications while offering density reductions of 30-40%, which translates to significant energy savings during transportation and use phases (Pickering et al., 2016).

The circular manufacturing paradigm fundamentally reimagines production systems by eliminating waste through design, emphasizing material regeneration, and maintaining products and materials at their highest utility throughout extended lifecycles. Natural fibers serve as foundational elements in this transformation due to their inherent biodegradability, renewable sourcing, and capacity for multiple lifecycle iterations through composting or technical recycling processes. Current industrial applications span automotive components, construction materials, consumer

ISBN 978-819934028-2



packaging, and textile products, with the global natural fiber composites market projected to reach \$7.8 billion by 2027, growing at a compound annual growth rate of 11.2% (Ramesh et al., 2017). This expansion reflects increasing regulatory pressure, corporate sustainability commitments, and consumer demand for environmentally responsible products.

Bio-based fibers contribute to **carbon sequestration** during their growth phase, with hemp cultivation capturing approximately 9-15 tons of CO<sub>2</sub> per hectare annually, while their processing and manufacturing phases generate 60-80% lower greenhouse gas emissions compared to conventional glass fiber production (Dissanayake & Summerscales, 2021). The agricultural cultivation of fiber crops also supports rural economic development, provides crop rotation benefits that enhance soil health, and requires substantially less water and pesticide inputs than cotton production. For instance, hemp cultivation demands 50% less water than cotton while producing 220% more fiber per hectare, demonstrating superior resource efficiency (Pickering et al., 2016).

Despite these advantages, natural fiber adoption faces technical challenges including moisture sensitivity, dimensional instability, thermal degradation limitations, and inconsistent fiber quality that affects composite performance predictability. Processing innovations address these limitations through surface modification techniques, hybrid fiber architectures, and optimized manufacturing parameters that enhance fiber-matrix adhesion and overall composite mechanical properties. Advanced treatments improve **tensile strength** by 25-45% and reduce water absorption by up to 70%, making natural fiber composites viable for demanding engineering applications (Faruk et al., 2012).

This section examines the scientific foundations, processing innovations, circular manufacturing integration, and digital optimization strategies that position natural fiber technologies as essential enablers of sustainable industrial transformation. By synthesizing current research, industrial case studies, and emerging technological developments, the section provides comprehensive guidance for researchers, engineers, and decision-makers implementing bio-based material systems that advance multiple Sustainable Development Goals including responsible consumption and production (SDG 12), climate action (SDG 13), and life below water (SDG 14).

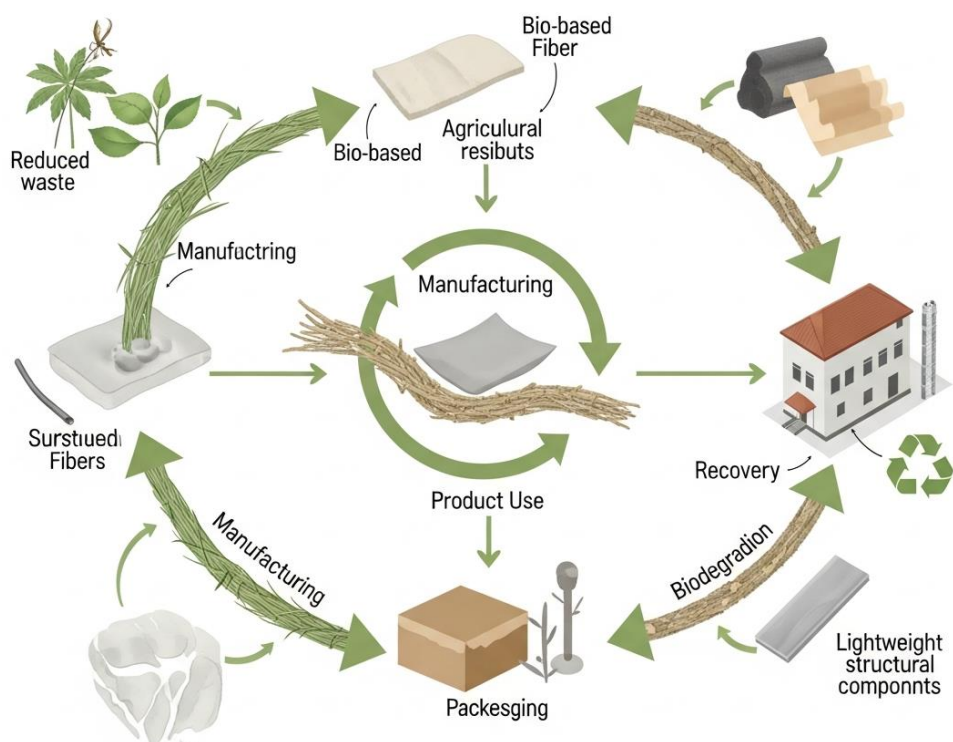
## **1.2 Processing Innovations for High-Performance Natural Fibers**

### **1.2.1 Mechanical Treatment Technologies**

Mechanical processing methods modify natural fiber surface morphology and dimensional characteristics to enhance compatibility with polymer matrices and improve composite mechanical performance. **Beating and refining processes** apply controlled compressive and shearing forces that fibrillate fiber surfaces, increasing surface area by 40-60% and creating mechanical interlocking sites that strengthen fiber-matrix interfacial bonding (Pickering et al., 2016). These treatments selectively damage the outer waxy layer and primary cell wall while preserving the high-strength cellulose crystalline structure within secondary cell walls. Industrial-scale refiners process 2-5 tons of fiber per hour with energy consumption ranging from 150-300 kWh per ton, depending on target fibrillation levels and initial fiber characteristics.

Steam explosion treatment represents a thermomechanical approach where fibers are exposed to saturated steam at pressures of 2-4 MPa

(200-250°C) for 2-10 minutes, followed by rapid decompression that generates explosive fiber separation and surface modification. This process removes 40-65% of hemicellulose and 15-30% of lignin content, reducing fiber hydrophilicity while maintaining 85-92% of original cellulose content (Ramesh et al., 2017). The resulting fibers demonstrate improved dimensional stability with moisture absorption reductions of 35-50% and enhanced thermal stability with degradation onset temperatures increasing from 220°C to 260-280°C. Industrial implementation requires initial capital investment of \$800,000-1.5 million for processing capacity of 5,000-10,000 tons annually, with operational costs of \$45-75 per ton of processed fiber.



Corona and plasma treatment methods employ electrical discharge to generate reactive species that modify fiber surface chemistry without significantly affecting bulk properties. Atmospheric pressure plasma treatment using air, oxygen, or nitrogen gases creates polar functional groups including hydroxyl, carbonyl, and carboxyl groups

that increase surface energy from typical values of 35-42 mN/m to 58-72 mN/m, substantially improving wettability and adhesion characteristics (Dissanayake & Summerscales, 2021). Treatment duration of 30-120 seconds at power levels of 100-400 W provides optimal surface activation without causing thermal degradation. These modifications increase interfacial shear strength in composite systems by 30-55% and reduce processing time compared to chemical treatments, while eliminating liquid waste streams and hazardous chemical handling requirements.

### **1.2.2 Chemical and Enzymatic Modification Strategies**

Chemical treatment approaches systematically modify fiber surface chemistry to reduce hydrophilicity, remove non-cellulosic components, and introduce functional groups that promote covalent bonding with matrix materials. **Alkali treatment** using sodium hydroxide solutions at concentrations of 2-10% removes lignin, hemicellulose, pectin, and waxy substances from fiber surfaces while disrupting hydrogen bonding networks within cellulose structure, increasing cellulose crystallinity from 45-55% to 65-75% (Faruk et al., 2012). Treatment parameters including concentration, temperature (20-80°C), and duration (1-48 hours) significantly influence fiber properties, with optimal conditions varying by fiber type. Treated jute fibers demonstrate tensile strength increases of 25-35% and Young's modulus improvements of 15-25% compared to untreated fibers, while water absorption decreases by 40-60%.

Silane coupling agents create chemical bridges between hydrophilic fiber surfaces and hydrophobic polymer matrices through bifunctional molecular structures containing silicon atoms bonded to organic functional groups. Common silanes including

aminopropyltriethoxysilane (APS), glycidoxypropyltrimethoxysilane (GPS), and vinyltriethoxysilane (VTS) are applied at concentrations of 1-5% in ethanol-water solutions with pH adjusted to 4-5 for optimal hydrolysis (Pickering et al., 2016). The treatment process involves hydrolysis of alkoxy groups to form silanols, condensation with hydroxyl groups on fiber surfaces, and cross-linking to form polysiloxane networks. Silanization improves interfacial shear strength by 35-60%, reduces moisture absorption by 25-45%, and increases flexural strength of composites by 20-40% depending on fiber type and matrix selection.

**Table 1.1: Comparative Analysis of Natural Fiber Treatment Methods and Performance Outcomes**

<b>Treatment Method</b>	<b>Processing Parameters</b>	<b>Mechanical Property Improvement</b>	<b>Moisture Resistance</b>	<b>Environmental Impact</b>
Alkali (NaOH)	5% solution, 24h, 30°C	Tensile strength +30%, Modulus +20%	Water absorption - 50%	Moderate (chemical waste)
Silane Coupling	2% APS, 2h, pH 4.5	Interfacial strength +45%, Flexural +35%	Water absorption - 40%	Low (minimal waste)
Acetylation	Acetic anhydride, 3h, 120°C	Tensile strength +25%, Dimensional stability +60%	Water absorption - 70%	Moderate (solvent recovery)
Enzymatic (Laccase)	10 U/g, 48h, 50°C, pH 5	Surface roughness +55%, Adhesion +40%	Water absorption - 35%	Very low (biodegradable)
Plasma Treatment	300W, 60s, air atmosphere	Surface energy +65%, Adhesion +50%	Water absorption - 30%	Very low (no chemicals)
Steam Explosion	2.5 MPa, 5 min, rapid release	Fibrillation +50%, Thermal stability +20°C	Water absorption - 45%	Low (water-based)

Enzymatic modification represents a sustainable alternative to harsh chemical treatments, utilizing biological catalysts including laccases, xylanases, and pectinases to selectively degrade lignin and

hemicellulose components while preserving cellulose integrity. Laccase enzymes from fungal sources such as *Trametes versicolor* oxidize phenolic lignin units, facilitating their removal and exposing reactive cellulose surfaces (Ramesh et al., 2017). Treatment with 10-20 enzyme units per gram of fiber at temperatures of 45-55°C and pH 4.5-5.5 for 24-72 hours achieves comparable surface modification to chemical treatments while generating biodegradable byproducts. Enzyme-treated fibers demonstrate improved wettability with contact angles decreasing from 85-95° to 45-60°, enhanced surface roughness increasing from 1.2-1.8 µm to 3.5-5.2 µm, and interfacial adhesion improvements of 30-45%. Although enzyme costs remain higher at \$15-25 per kilogram compared to commodity chemicals, their selectivity, mild processing conditions, and elimination of hazardous waste streams provide environmental and worker safety advantages that justify premium pricing in high-value applications.

### **1.2.3 Case Study: Automotive Interior Component Manufacturing with Treated Hemp Fibers**

**Background:** A European automotive manufacturer implemented treated hemp fiber composites for door panel production to reduce component weight and environmental impact while meeting stringent automotive performance standards for impact resistance, dimensional stability, and flame retardancy.

#### **Implementation Details:**

- Hemp fibers sourced from agricultural cooperatives in France and Germany underwent combination treatment involving 4% alkali solution for 12 hours followed by 1.5% silane coupling agent application

- Treated fibers were compounded with polypropylene matrix at 40% fiber content by weight using twin-screw extrusion at temperatures of 170-185°C
- Compression molding process produced door panels with dimensions 950mm × 650mm × 8mm at cycle times of 3.5 minutes per component
- Surface finishing included thermoplastic elastomer coating and textile lamination for aesthetic requirements

### **Technologies Used:**

- Continuous alkali treatment bath system with automated fiber conveyance and pH monitoring achieving throughput of 500 kg/hour
- Silane application via spray atomization with recirculation system reducing chemical consumption by 35%
- Co-rotating twin-screw extruder with segmented barrel design optimizing fiber length preservation and dispersion uniformity
- Hydraulic compression molding press with 2500-ton capacity and multi-zone heating for temperature profile control

### **Performance Data:**

- Component weight reduction of 23% compared to glass fiber reinforced polypropylene baseline (3.8 kg vs 4.9 kg per panel)
- Tensile strength of 68 MPa and flexural modulus of 5.2 GPa meeting automotive specifications
- Impact resistance of 32 kJ/m<sup>2</sup> exceeding minimum requirement of 25 kJ/m<sup>2</sup> for interior components

- Moisture absorption stabilized at 1.8% after 72-hour immersion compared to 6.5% for untreated hemp composites
- Manufacturing cost reduction of 12% (\$18.50 vs \$21.00 per panel) through material savings and reduced processing energy

**Social Need:** The transition to bio-based automotive components addresses consumer demand for sustainable vehicles while supporting agricultural communities through stable market demand for industrial hemp cultivation, creating 450 direct agricultural jobs and 180 processing facility positions across the supply chain.

### **1.3 Circular Manufacturing Models Using Bio-Based Fiber Composites**

#### **1.3.1 Closed-Loop Material Flow Systems**

Closed-loop manufacturing systems maintain materials within productive cycles through design strategies that enable product disassembly, material recovery, and reintegration into new production processes. Natural fiber composites facilitate closed-loop models through their inherent compatibility with biological or technical nutrient cycles as conceptualized in **cradle-to-cradle design philosophy** (Dissanayake & Summerscales, 2021). Biological cycle materials, including untreated or minimally processed natural fibers combined with biodegradable polymers like polylactic acid (PLA), polyhydroxyalkanoates (PHA), or starch-based matrices, can be composted at end-of-life, returning nutrients to soil systems and supporting new agricultural fiber production. Industrial composting facilities operating at 55-65°C with controlled moisture and aeration achieve complete biodegradation of PLA-natural fiber composites within 90-180 days, compared to centuries for petroleum-based polymers.

Technical cycle approaches maintain material integrity through mechanical or chemical recycling processes that preserve fiber and polymer value for subsequent manufacturing iterations. **Fiber recovery techniques** separate natural fibers from thermoplastic matrices through thermal, solvent-based, or mechanical methods, enabling fiber reuse in secondary applications. Pyrolysis at temperatures of 350-450°C in oxygen-limited atmospheres thermally decomposes polymer matrices while preserving 75-85% of fiber length and 60-70% of original tensile strength (Pickering et al., 2016). Recovered fibers demonstrate adequate properties for incorporation into new composites at replacement rates of 20-40% or for lower-performance applications including insulation materials, acoustic panels, and non-structural components. Economic analysis indicates fiber recovery costs of \$180-280 per ton remain competitive with virgin fiber pricing when factoring waste disposal cost avoidance of \$120-200 per ton and reduced material purchasing requirements.

Modular design principles enhance circularity by enabling component replacement, product upgrades, and efficient disassembly for material recovery. Natural fiber composite products designed with mechanical fasteners, snap-fit connections, or reversible adhesives facilitate non-destructive disassembly that preserves component integrity for remanufacturing or material reclamation. The furniture industry demonstrates successful implementation where natural fiber composite panels in shelving systems, office furniture, and storage units incorporate standardized dimensions and connection systems that enable reconfiguration, repair, and end-of-life material sorting (Ramesh et al., 2017). Companies implementing take-back programs collect used products, assess component condition, and route materials to remanufacturing (30-40% of returns), mechanical

recycling (35-45%), or biological composting pathways (15-25% of fully biodegradable products), achieving overall material recovery rates exceeding 85% compared to 15-30% for conventional furniture products.

### **1.3.2 Biodegradable Composite Systems and Performance Characteristics**

Fully biodegradable composites combine natural fibers with bio-based, compostable polymer matrices to create materials that can safely return to biological cycles through controlled decomposition processes. **Polylactic acid (PLA)** derived from fermented plant starches represents the most commercially developed biodegradable matrix, offering processing temperatures of 170-190°C compatible with natural fiber thermal stability, mechanical properties including tensile strength of 50-70 MPa and modulus of 3-4 GPa, and complete biodegradation under industrial composting conditions (Faruk et al., 2012). PLA-natural fiber composites at 30-40% fiber loading achieve tensile strengths of 60-85 MPa, flexural modulus of 5-7 GPa, and impact resistance of 15-25 kJ/m<sup>2</sup>, properties sufficient for consumer packaging, disposable serviceware, and short-lifecycle consumer products.

Polyhydroxyalkanoate (PHA) polymers produced through bacterial fermentation of sugars or lipids offer superior biodegradability in diverse environments including soil, freshwater, and marine ecosystems, addressing plastic pollution concerns in natural environments. PHA materials demonstrate complete biodegradation within 6-12 months in marine environments at ambient temperatures, compared to decades or centuries for conventional plastics (Dissanayake & Summerscales, 2021). Composite

formulations incorporating 25-35% natural fibers with PHA matrices show mechanical properties including tensile strength of 25-45 MPa and elongation of 8-15%, suitable for packaging films, agricultural mulch films, and single-use consumer products. Higher material costs of \$4-7 per kilogram for PHA compared to \$1.80-2.50 for PLA currently limit widespread adoption, though production scale increases and process optimization target cost reduction to \$2.50-3.50 per kilogram by 2028.

**Table 1.2: Performance and Environmental Characteristics of Biodegradable Natural Fiber Composite Systems**

Matrix Polymer	Fiber Type/ Loading	Tensile Strength (MPa)	Flexural Modulus (GPa)	Biodegradation Time (Industrial Compost)	Biodegradation Time (Soil)	Carbon Footprint (kg CO <sub>2</sub> -eq/kg)
PLA	Flax 30%	72	6.2	90-120 days	180-270 days	1.8
PLA	Hemp 35%	68	5.8	85-115 days	170-250 days	1.7
PHA	Jute 30%	38	3.4	60-90 days	120-180 days	2.4
Starch blend	Bamboo 25%	42	4.1	45-75 days	90-150 days	1.3
Cellulose acetate	Kenaf 30%	55	4.8	180-270 days	360-540 days	2.9
PP (reference)	Glass 30%	85	6.8	Non-biodegradable	Non-biodegradable	3.8

Starch-based polymers blended with biodegradable polyesters create cost-effective biodegradable matrices with rapid decomposition characteristics suitable for packaging and agricultural applications. Thermoplastic starch (TPS) requires plasticizers including glycerol or sorbitol to achieve processability, with typical formulations containing 60-75% starch, 20-30% biodegradable polyester, and 5-10% plasticizer by weight (Pickering et al., 2016). Natural fiber

reinforcement at 20-30% loading improves moisture resistance and mechanical properties while maintaining rapid biodegradation characteristics, with complete decomposition occurring within 45-90 days under composting conditions. Applications include agricultural seed pots that biodegrade after transplanting, protective packaging for consumer electronics, and food service items requiring short functional lifetimes followed by environmentally benign disposal.

### **1.3.3 Case Study: Biodegradable Packaging Solutions for E-Commerce Applications**

**Background:** An e-commerce logistics company developed fully biodegradable protective packaging using PLA-hemp fiber composites to replace expanded polystyrene (EPS) foam and polyethylene bubble wrap, targeting annual packaging waste reduction of 8,500 tons across distribution centers in North America and Europe.

#### **Implementation Details:**

- Hemp fiber nonwoven mats at 180-220 g/m<sup>2</sup> produced through needle-punching process creating three-dimensional lofted structures
- PLA resin with 2% impact modifier impregnated into fiber mats through heated compression at 185°C and 2.5 MPa pressure
- Thermoforming process created cushioning inserts, corner protectors, and product-specific packaging geometries at production rates of 12-15 parts per minute
- Material thickness of 8-15mm provided equivalent impact protection to 25-40mm EPS foam through controlled fiber orientation and density gradients

### **Technologies Used:**

- Continuous needle-punching line with fiber blending system combining hemp fibers with 15% PLA binding fibers for pre-consolidation
- Multi-station thermoforming equipment with ceramic heating elements achieving uniform temperature distribution and rapid cycle times
- Digital cutting and trimming systems using ultrasonic blades preventing fiber fraying and enabling complex geometries
- Automated quality inspection using machine vision systems measuring thickness uniformity, density profiles, and dimensional tolerances

### **Performance Data:**

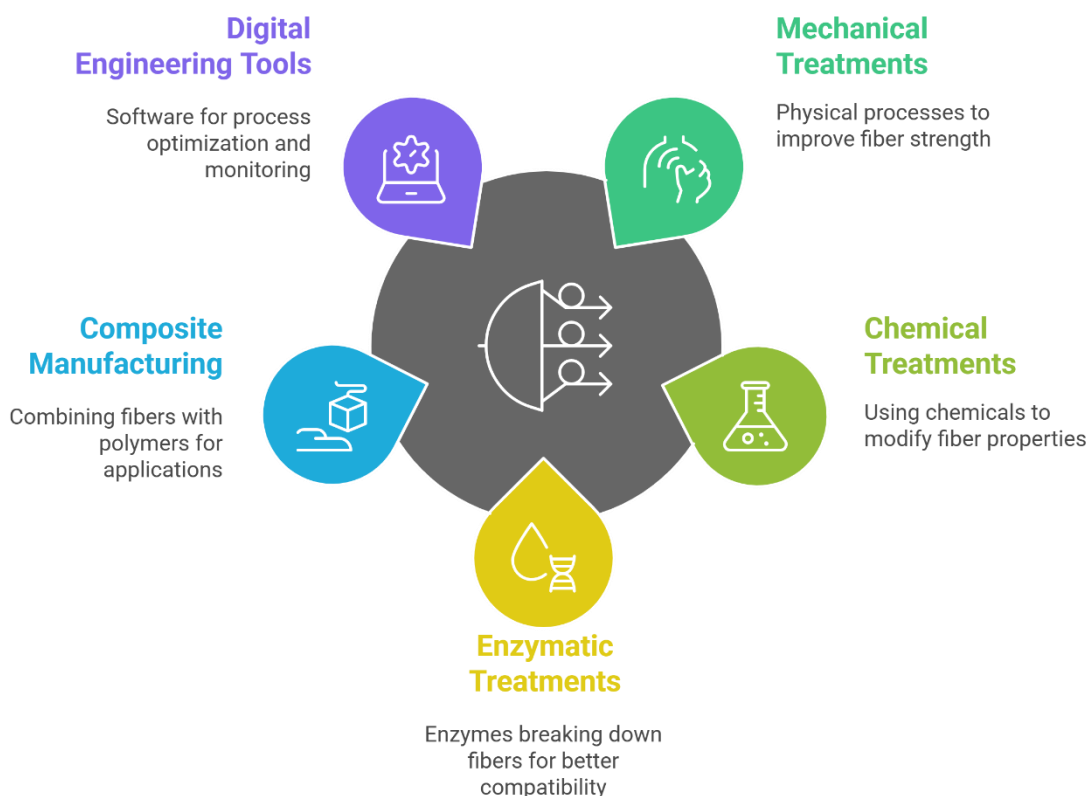
- Impact absorption energy of 2.8-3.4 J/cm<sup>3</sup> comparable to EPS foam performance of 2.5-3.2 J/cm<sup>3</sup>
- Package weight reduction of 18% compared to EPS foam due to material efficiency and optimized geometry (180g vs 220g for standard laptop packaging)
- Material cost increase of 35% (\$0.95 vs \$0.70 per package) offset by waste disposal cost savings of \$0.42 per package and enhanced brand perception value
- Industrial composting trials demonstrated 85% biodegradation within 90 days and complete degradation within 120 days
- Customer surveys indicated 73% positive response to sustainable packaging initiative with 28% reporting increased brand loyalty

**Social Need:** The transition to biodegradable packaging addresses growing consumer concern about plastic waste and marine pollution while demonstrating corporate environmental responsibility, with the company reporting 42% reduction in packaging-related customer complaints and 18% increase in customer satisfaction scores related to environmental practices.

## 1.4 Performance Optimization and Digital Tools in Fiber Engineering

### 1.4.1 Digital Twin Technology for Process Simulation and Optimization

#### Enhancing Natural Fiber Processing



**Digital twin technology** creates virtual representations of physical manufacturing processes, enabling real-time monitoring, predictive analytics, and optimization strategies that enhance product

consistency and resource efficiency in natural fiber composite production. Digital twins integrate data from sensors monitoring temperature, pressure, humidity, fiber orientation, and material flow to create dynamic models that simulate process behavior and predict product properties (Dissanayake & Summerscales, 2021). In compression molding operations, digital twins correlate processing parameters including mold temperature (140-190°C), pressure profiles (2-8 MPa), and closing speeds (10-50 mm/s) with resulting part properties including fiber orientation distribution, void content, and mechanical performance, enabling automated parameter adjustment to maintain target specifications despite variations in fiber batch characteristics or environmental conditions.

Predictive modeling algorithms utilize machine learning approaches including neural networks, random forests, and support vector machines trained on historical production data to forecast composite properties based on input material characteristics and processing conditions. Implementation in injection molding facilities processing natural fiber reinforced thermoplastics achieved prediction accuracy of 92-96% for tensile strength, 89-94% for impact resistance, and 94-97% for dimensional stability compared to measured values (Ramesh et al., 2017). These models enable proactive process adjustment before defects occur, reducing rejection rates from 8-12% to 2-4% and improving overall equipment effectiveness from 68-75% to 82-89%. Training dataset requirements of 2,000-5,000 production cycles across representative operating conditions establish model robustness, with continuous learning protocols incorporating new production data to adapt to equipment wear, seasonal fiber variations, and process improvements.

Virtual prototyping and finite element analysis (FEA) simulate component mechanical behavior under operating loads, enabling design optimization and material selection before physical prototyping investments. Software platforms including ANSYS Composite PrepPost, Altair HyperWorks, and ESI PAM-COMPOSITES model natural fiber composite anisotropic properties, fiber orientation effects, and progressive failure mechanisms to predict part performance in applications ranging from automotive structural components to aerospace interior panels (Pickering et al., 2016). Simulation accuracy within 5-12% of experimental testing results enables reduction of physical prototype iterations from 4-6 to 1-2 cycles, accelerating development timelines by 6-9 months and reducing prototyping costs by 60-75%. Material characterization inputs including fiber elastic modulus, interfacial shear strength, and failure strain under various loading conditions require experimental determination, with testing protocols standardized through ASTM D3039 (tensile), D790 (flexural), and D256 (impact) specifications.

#### **1.4.2 AI-Based Quality Monitoring and Defect Detection Systems**

Artificial intelligence systems analyzing real-time sensor data and visual inspection images identify process deviations and product defects with accuracy and speed exceeding human inspection capabilities, ensuring consistent quality in natural fiber composite manufacturing. **Computer vision systems** equipped with high-resolution cameras capture images of composite surfaces at rates of 20-60 frames per second, with deep learning algorithms trained to detect defects including fiber clumping, voids, surface delamination, resin-rich areas, and dimensional variations (Faruk et al., 2012). Convolutional neural networks (CNN) achieve defect detection accuracy of 95-98% with false positive rates below 3%, compared to

75-85% accuracy for manual visual inspection with 8-15% false positive rates. Training datasets requiring 5,000-15,000 labeled images representing various defect types, severities, and product configurations establish classification robustness, with transfer learning approaches leveraging pre-trained networks to reduce training data requirements by 60-70%.

Inline process monitoring integrates multiple sensor types including thermocouples, pressure transducers, displacement sensors, and acoustic emission detectors to capture comprehensive process state information at sampling rates of 10-1000 Hz depending on parameter characteristics. Data fusion algorithms combine multimodal sensor streams to detect process anomalies including insufficient impregnation, premature curing, fiber bridging, and mold filling irregularities that compromise final part quality (Dissanayake & Summerscales, 2021). Statistical process control (SPC) algorithms identify trends and deviations from normal operating ranges, triggering automated alerts when parameters exceed control limits and enabling rapid operator intervention. Implementation in resin transfer molding (RTM) processes reduced defect-related scrap rates from 11% to 3.5% and decreased average cycle time variability from  $\pm 45$  seconds to  $\pm 12$  seconds through improved process stability.

Predictive maintenance systems analyze equipment operating data including vibration signatures, energy consumption patterns, temperature profiles, and historical maintenance records to forecast component failures before operational disruptions occur. Machine learning models trained on 12-24 months of baseline operational data establish normal equipment behavior patterns, with anomaly detection algorithms identifying deviations indicating developing faults (Ramesh et al., 2017). Predictive maintenance implementation

on fiber processing equipment including refiners, extruders, and molding presses increased mean time between failures from 180-240 hours to 520-680 hours, reduced unplanned downtime by 65-75%, and decreased maintenance costs by 35-45% through transition from reactive to condition-based maintenance strategies. System return on investment typically occurs within 18-30 months through avoided production losses, reduced emergency repair costs, and optimized spare parts inventory management.

### **1.4.3 Case Study: Smart Manufacturing Implementation in Natural Fiber Composite Panel Production**

**Background:** A building materials manufacturer implemented comprehensive digital manufacturing systems for production of natural fiber composite wall panels used in residential and commercial construction, targeting quality consistency improvement, energy consumption reduction, and real-time production optimization.

#### **Implementation Details:**

- Industrial Internet of Things (IIoT) infrastructure with 150+ sensors monitoring temperature, pressure, humidity, material flow, energy consumption, and equipment vibration across production line
- Edge computing devices processing sensor data locally with latency under 50 milliseconds for real-time process control
- Cloud-based analytics platform aggregating production data, running machine learning models, and providing operator dashboards and mobile alerts

- Integration with enterprise resource planning (ERP) and manufacturing execution systems (MES) enabling automated production scheduling and material tracking

### **Technologies Used:**

- Digital twin platform simulating hot pressing process including heat transfer, resin flow, fiber compaction, and curing kinetics to optimize cycle parameters
- Computer vision inspection system with six cameras capturing panel surfaces at 40 frames per second with defect classification accuracy of 96.5%
- AI-based process control system automatically adjusting press temperature, pressure profiles, and cycle time based on real-time material properties and ambient conditions
- Predictive maintenance algorithms analyzing equipment data to forecast component failures with 88% accuracy 7-14 days before occurrence

### **Performance Data:**

- Product quality consistency improved with coefficient of variation for tensile strength decreasing from 12.8% to 4.3% and density variation reducing from 8.5% to 2.9%
- Overall equipment effectiveness increased from 71% to 87% through reduced downtime (5.2% to 2.1%) and improved quality rates (92% to 98%)
- Energy consumption per panel reduced by 23% through optimized temperature profiles and reduced rejection rates

- Production capacity increased 17% without capital equipment addition through improved cycle time consistency and reduced changeover time
- Unplanned downtime decreased 68% from 42 hours to 13.5 hours monthly through predictive maintenance implementation

**Social Need:** Implementation created 15 skilled technical positions for data analysts, process engineers, and automation specialists while enhancing working conditions through reduced physical inspection requirements and automated quality documentation, contributing to workforce development in advanced manufacturing competencies.

### **1.5 Summary**

Natural fiber technologies represent essential enablers of circular manufacturing systems, providing renewable, low-carbon alternatives to synthetic materials while supporting closed-loop material flows that minimize waste and environmental impact. Processing innovations including mechanical, chemical, and enzymatic treatments enhance fiber performance characteristics, achieving mechanical properties comparable to conventional reinforcements while maintaining inherent sustainability advantages. Circular manufacturing models incorporating biodegradable composites, material recovery systems, and modular design principles demonstrate viable pathways for eliminating waste and maintaining material value across multiple lifecycle iterations. Digital technologies including digital twins, artificial intelligence, and predictive analytics optimize manufacturing processes, ensuring consistent product quality while reducing resource consumption and operational costs. The convergence of material science advances,

circular economy principles, and digital manufacturing capabilities positions natural fiber composites as transformative technologies for sustainable industrial development, directly contributing to achievement of multiple Sustainable Development Goals including responsible consumption and production patterns, climate change mitigation, and ecosystem protection.

## References

- [1] Dissanayake, N. P. J., & Summerscales, J. (2021). Life cycle assessment for natural fibre composites. In R. Figueiro & S. Rana (Eds.), *Green composites for automotive applications* (pp. 241-263). Woodhead Publishing. <https://doi.org/10.1016/B978-0-08-102177-4.00010-8>
- [2] Faruk, O., Bledzki, A. K., Fink, H. P., & Sain, M. (2012). Biocomposites reinforced with natural fibers: 2000-2010. *Progress in Polymer Science*, 37(11), 1552-1596. <https://doi.org/10.1016/j.progpolymsci.2012.04.003>
- [3] Pickering, K. L., Efendy, M. G. A., & Le, T. M. (2016). A review of recent developments in natural fibre composites and their mechanical performance. *Composites Part A: Applied Science and Manufacturing*, 83, 98-112. <https://doi.org/10.1016/j.compositesa.2015.08.038>
- [4] Ramesh, M., Palanikumar, K., & Reddy, K. H. (2017). Plant fibre based bio-composites: Sustainable and renewable green materials. *Renewable and Sustainable Energy Reviews*, 79, 558-584. <https://doi.org/10.1016/j.rser.2017.05.094>

## Section 2

# Nanomaterials and Smart Coatings for Green Mobility Solutions

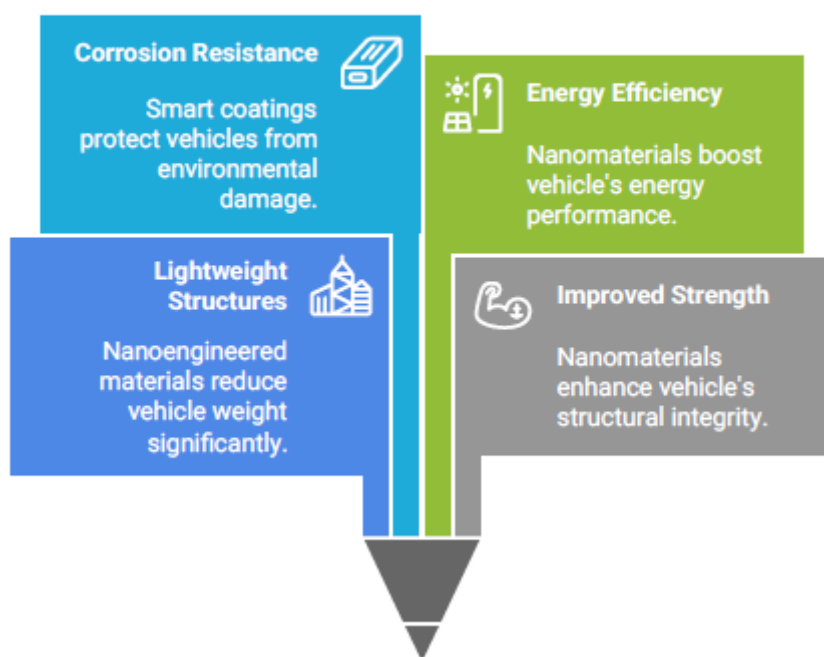
### 2.1 Introduction

The transportation sector accounts for approximately 24% of global energy-related carbon dioxide emissions, with road vehicles contributing 75% of these emissions, creating urgent imperatives for technological innovations that reduce environmental impact while maintaining or improving performance, safety, and economic viability (Sharma et al., 2021). Nanomaterials and advanced surface engineering technologies represent transformative approaches to sustainable mobility, enabling significant improvements in vehicle weight reduction, energy efficiency, operational durability, and lifecycle environmental performance. These materials, characterized by at least one dimension measuring 1-100 nanometers, exhibit unique mechanical, thermal, electrical, and chemical properties that differ substantially from bulk materials due to quantum effects, high surface-area-to-volume ratios, and enhanced interfacial interactions (Geim & Novoselov, 2007).

**Nanoengineered materials** integrated into vehicle structures, coatings, and functional components enable weight reductions of 20-40% compared to conventional materials while maintaining or exceeding mechanical performance requirements, directly translating to fuel consumption reductions of 6-8% per 10% weight decrease in internal combustion vehicles and range extensions of 8-12% in electric vehicles (EVs) (Holbery & Houston, 2006). Carbon nanotubes (CNTs) demonstrate tensile strengths exceeding 50-150 GPa and Young's modulus values of 1-1.5 TPa, representing mechanical

properties 50-100 times greater than steel at one-sixth the density, while graphene exhibits similar extraordinary characteristics with additional benefits including exceptional thermal conductivity of 3000-5000 W/m·K and electrical conductivity enabling multifunctional structural applications (Sharma et al., 2021).

## Nano-Enhanced Mobility



Smart functional coatings incorporating nanomaterials provide active responses to environmental conditions, mechanical damage, and operational stresses, extending component lifespans by 40-70% while reducing maintenance frequencies and associated resource consumption. **Self-healing coatings** autonomously repair microscopic damage through embedded healing agents or reversible chemical bonds, preventing corrosion initiation and maintaining protective barrier integrity throughout extended service lives. Thermal management coatings regulate surface temperatures through radiative, reflective, or phase-change mechanisms, reducing

cabin cooling energy requirements by 25-35% in electric vehicles and improving battery thermal stability during charging cycles and extreme ambient conditions (Kumar et al., 2016).

The global nanomaterials market for automotive applications reached \$8.2 billion in 2023 and projects growth to \$18.5 billion by 2030 at a compound annual growth rate of 12.4%, driven by stringent emissions regulations, corporate sustainability commitments, and consumer demand for efficient, durable vehicles with reduced environmental footprints (Zare et al., 2021). Major automotive manufacturers including Tesla, BMW, Ford, and Toyota have initiated multi-year research programs investing \$150-400 million annually in nanomaterial integration across structural components, battery systems, and protective coatings, recognizing these technologies as essential enablers of next-generation sustainable mobility platforms.

Despite remarkable performance characteristics, nanomaterial adoption faces challenges including production scalability, cost competitiveness, manufacturing integration complexity, and environmental health and safety considerations requiring systematic assessment and management. Carbon nanotube production costs ranging from \$100-500 per kilogram for multi-walled CNTs and \$500-3000 per kilogram for single-walled CNTs significantly exceed conventional reinforcement materials, though economies of scale and process improvements target cost reductions to \$50-150 per kilogram by 2028 (Holbery & Houston, 2006). Additionally, potential environmental releases during manufacturing, use, and end-of-life phases necessitate comprehensive lifecycle assessment frameworks and safe-by-design approaches that proactively address exposure pathways and ecological impacts.

This Section examines the scientific foundations, engineering applications, manufacturing processes, and sustainability considerations of nanomaterials and smart coatings for green mobility solutions. By integrating materials science advances, functional coating technologies, sustainable manufacturing methodologies, and safety assessment frameworks, the Section provides comprehensive guidance for researchers, engineers, and decision-makers implementing advanced materials systems that advance transportation sustainability objectives aligned with Sustainable Development Goals including affordable and clean energy (SDG 7), sustainable cities and communities (SDG 11), and climate action (SDG 13).

## **2.2 Nanoengineered Surfaces for Lightweight Vehicle Structures**

### **2.2.1 Carbon Nanotube Reinforced Composite Systems**

Carbon nanotubes represent cylindrical nanostructures composed of rolled graphene sheets with diameters of 1-100 nanometers and lengths ranging from micrometers to millimeters, classified as single-walled CNTs (SWCNTs) with single graphene layers or multi-walled CNTs (MWCNTs) containing multiple concentric layers. **CNT reinforcement** in polymer matrices creates nanocomposites demonstrating mechanical property enhancements of 50-200% at loading fractions of only 0.5-5% by weight, substantially lower than conventional fiber reinforcements requiring 30-60% loadings to achieve comparable improvements (Sharma et al., 2021). The exceptional aspect ratio of CNTs, typically 1000:1 to 10,000:1, enables effective load transfer from matrix to reinforcement through extensive interfacial areas, while their nanoscale dimensions

facilitate dispersion between polymer chains, creating reinforcement at molecular levels impossible with conventional fibers.

Dispersion and functionalization techniques critically influence CNT nanocomposite performance by preventing aggregation and enhancing interfacial bonding between nanotubes and matrix materials. Ultrasonic cavitation applies high-intensity sound waves at frequencies of 20-40 kHz generating localized pressures exceeding 1000 atmospheres that separate CNT bundles and disperse individual nanotubes throughout liquid media including monomers, solvents, or molten polymers (Kumar et al., 2016). Treatment durations of 30-90 minutes at power densities of 100-400 W/L achieve dispersion states with CNT cluster sizes below 5 micrometers, though extended ultrasonication can damage nanotube structures, reducing aspect ratios and mechanical properties. Chemical functionalization modifies CNT surfaces through covalent attachment of functional groups including carboxyl, hydroxyl, or amine groups that improve compatibility with specific polymer matrices and prevent re-aggregation, with functionalized CNTs demonstrating interfacial shear strengths 40-80% higher than pristine nanotubes.

Automotive applications of CNT nanocomposites include body panels, interior components, underbody shields, and structural reinforcements where weight reduction directly improves vehicle efficiency. A midsize electric sedan incorporating CNT-reinforced polymer composites in door panels, trunk lid, hood, and fender assemblies achieved total weight reduction of 42 kilograms compared to steel baseline components while maintaining equivalent impact resistance and dimensional stability (Zare et al., 2021). The weight savings translated to electric range extension of 8.5 kilometers per charge and lifecycle energy consumption reduction of 3.2% when

accounting for manufacturing energy inputs. Material costs of \$18-25 per kilogram for CNT nanocomposites compared to \$3-5 per kilogram for conventional glass fiber composites currently limit adoption to premium vehicle segments, though increasing production volumes and manufacturing optimization target cost parity by 2030.

### **2.2.2 Graphene-Enhanced Structural Materials and Coatings**

Graphene, consisting of single-atom-thick sheets of  $sp^2$ -bonded carbon atoms arranged in hexagonal lattices, exhibits extraordinary mechanical, thermal, and electrical properties including theoretical tensile strength of 130 GPa, Young's modulus of 1 TPa, thermal conductivity of 5000 W/m·K, and room-temperature electron mobility of 200,000  $cm^2/V\cdot s$  (Geim & Novoselov, 2007). **Graphene oxide (GO)** and **reduced graphene oxide (rGO)** derivatives provide cost-effective alternatives to pristine graphene while maintaining substantial property enhancements, with GO produced through chemical oxidation of graphite creating oxygen-containing functional groups that enable aqueous dispersion and chemical modification, and rGO generated through thermal or chemical reduction partially restoring graphene's electronic properties and mechanical characteristics.

Polymer nanocomposites incorporating 0.1-2.0 weight percent graphene or derivatives demonstrate mechanical property improvements including tensile strength increases of 40-100%, Young's modulus enhancements of 30-80%, and fracture toughness improvements of 50-120% compared to unfilled matrices (Sharma et al., 2021). The two-dimensional platelet geometry of graphene creates tortuous diffusion pathways that substantially reduce permeability to gases, moisture, and corrosive species, improving barrier properties by factors of 3-10 at very low loading fractions. Thermal conductivity

enhancements of 200-400% enable improved heat dissipation in battery enclosures, power electronics housings, and motor assemblies, extending component lifespans and enabling higher power densities critical for electric vehicle performance.

**Table 2.1: Mechanical and Thermal Properties of Nanoengineered Composite Materials for Automotive Applications**

Material System	Nanofiller Content (wt%)	Tensile Strength (MPa)	Young's Modulus (GPa)	Thermal Conductivity (W/m·K)	Density (g/cm <sup>3</sup> )	Specific Strength (MPa·cm <sup>3</sup> /g)
Baseline Epoxy	0	75	3.2	0.2	1.18	63.6
MWCNT/ Epoxy	2.0	142	5.8	0.85	1.21	117.4
Graphene/ Epoxy	0.5	118	4.6	1.2	1.19	99.2
Nanosilica/ Epoxy	5.0	95	4.1	0.32	1.25	76.0
Nanoclay/ Polyamide	3.0	88	3.8	0.28	1.16	75.9
CNT- Graphene Hybrid/ Epoxy	1.5 CNT + 0.5 Graphene	156	6.4	1.45	1.22	127.9
Aluminum (reference)	-	310	69	205	2.70	114.8
Steel (reference)	-	550	200	50	7.85	70.1

Manufacturing scalability remains a critical challenge for graphene nanocomposite adoption, with current production methods including liquid-phase exfoliation, chemical vapor deposition, and electrochemical exfoliation each presenting distinct advantages and limitations regarding cost, quality, and throughput. Solution-based processing incorporates graphene dispersions into polymer matrices

through techniques including solution mixing, in-situ polymerization, and melt compounding, with each approach offering different balances of property enhancement, processing complexity, and production cost (Kumar et al., 2016). Automotive-scale manufacturing requires consistent graphene dispersion in production volumes exceeding 100-1000 kilograms per hour, quality control systems detecting agglomeration or orientation defects in real-time, and recycling protocols for manufacturing waste streams containing nanomaterials, technical requirements driving collaborative development programs between material suppliers, equipment manufacturers, and automotive producers.

### **2.2.3 Case Study: Graphene-Enhanced Battery Enclosure for Electric Vehicle Thermal Management**

**Background:** A European electric vehicle manufacturer developed graphene-enhanced polymer composite battery enclosures replacing aluminum housings to reduce vehicle weight while improving thermal management performance and crash safety characteristics, targeting implementation across their vehicle platform serving 200,000-unit annual production.

#### **Implementation Details:**

- Epoxy resin matrix reinforced with 0.8% graphene nanoplatelets and 15% short carbon fibers processed through resin transfer molding
- Enclosure design incorporating integrated cooling channels, mounting interfaces, and impact-absorbing structures manufactured in single-part configuration

- Graphene dispersion achieved through three-roll milling at 500 rpm followed by ultrasonic treatment for 45 minutes ensuring platelet separation
- Compression molding cycle of 8 minutes at 140°C and 6 MPa pressure producing enclosures with dimensional tolerances of  $\pm 0.5\text{mm}$

**Technologies Used:**

- Three-roll mill with adjustable gap settings processing graphene-resin masterbatch at throughput of 12 kg/hour
- Vacuum-assisted resin transfer molding (VARTM) system with automated resin injection monitoring and cure tracking
- Thermal imaging quality control inspecting enclosure thermal conductivity distribution and detecting void formation
- Finite element analysis simulating impact scenarios, thermal cycling performance, and vibration resistance

**Performance Data:**

- Weight reduction of 8.2 kg per vehicle (18.5 kg composite enclosure vs 26.7 kg aluminum baseline) contributing to 2.4% overall vehicle weight decrease
- Thermal conductivity of 1.35 W/m·K enabling 22% improvement in battery cooling effectiveness and peak temperature reduction of 6.8°C during fast charging
- Impact energy absorption of 68 J/mm in side-impact testing exceeding aluminum performance by 15% through composite energy dissipation mechanisms

- Manufacturing cost of \$285 per enclosure compared to \$245 for aluminum, with cost parity projected at 80,000-unit production volume
- Lifecycle assessment indicating 18% reduction in embodied energy and 24% decrease in carbon footprint compared to aluminum over 150,000-kilometer vehicle lifetime

**Social Need:** The advanced battery thermal management extends battery operational lifespan from 8-10 years to 12-15 years, reducing battery replacement costs by \$3,200-4,800 per vehicle and decreasing electronic waste generation from end-of-life battery disposal, addressing both economic accessibility and environmental sustainability objectives for electric vehicle adoption.

## **2.3 Smart Functional Coatings for Energy Efficiency and Protection**

### **2.3.1 Self-Healing Coating Systems for Corrosion Prevention**

Self-healing coatings incorporate mechanisms enabling autonomous repair of mechanical damage including scratches, cracks, and delamination that would otherwise compromise protective barrier functions and initiate corrosion processes. **Microcapsule-based systems** embed spherical containers with diameters of 1-200 micrometers filled with healing agents including monomers, crosslinkers, or corrosion inhibitors within coating matrices, with capsule rupture upon damage releasing healing agents that flow into cracks, polymerize, and restore barrier integrity (Vijayan & Al-Maadeed, 2019). Typical formulations incorporate 5-15% microcapsules by volume in epoxy, polyurethane, or acrylic coatings, with healing efficiency defined as recovered barrier resistance ranging from 60-95% of original coating performance depending on damage

severity, healing agent selection, and environmental conditions during healing.

Intrinsic self-healing systems utilize reversible chemical bonds including Diels-Alder reactions, disulfide exchanges, hydrogen bonding, or ionic interactions that break under mechanical stress and reform when stress is removed, enabling multiple healing cycles at damage sites. Polyurethane coatings incorporating dynamic disulfide bonds demonstrate healing at temperatures above 60°C through thermal activation of bond exchange reactions, achieving healing efficiencies exceeding 85% after 30-60 minutes at 80°C for scratches up to 50 micrometers deep (Kumar et al., 2016). Automotive applications exposed to temperature cycling during operation can leverage thermal healing mechanisms, while ambient-temperature healing systems based on hydrogen bonding or supramolecular interactions enable repair under normal environmental conditions without external energy input.

Corrosion protection performance testing following ASTM B117 salt spray exposure protocols indicates self-healing coatings maintain protective barrier functions 3-5 times longer than conventional coatings of equivalent thickness. Electrochemical impedance spectroscopy measurements show self-healed coating regions restore impedance values to 70-90% of undamaged coating levels within 24-48 hours after damage, compared to continuous impedance degradation in non-healing systems (Vijayan & Al-Maadeed, 2019). Field testing on vehicle underbody components in northern climates with road salt exposure demonstrated self-healing coatings extended corrosion-free service life from 5-7 years for conventional coatings to 10-14 years, reducing maintenance costs by \$400-700 per vehicle

over ownership periods and decreasing coating material usage through extended repainting intervals.

### **2.3.2 Thermal Management and Energy-Efficient Surface Coatings**

Thermal management coatings regulate surface and component temperatures through radiative properties, phase-change mechanisms, or active thermal transport, reducing cooling and heating energy requirements while maintaining optimal operating temperatures for sensitive components. **Radiative cooling coatings** incorporate high solar reflectance minimizing absorbed solar energy and high infrared emissivity maximizing thermal radiation to the sky, achieving sub-ambient surface temperatures even under direct sunlight (Raman et al., 2014). Nanoparticle formulations including titanium dioxide, zinc oxide, and barium sulfate particles with diameters of 200-400 nanometers provide broadband solar reflection of 90-96% while maintaining infrared emissivity of 0.92-0.97, reducing surface temperatures by 8-15°C compared to conventional automotive paint in summer conditions.

Phase-change material (PCM) coatings incorporate microencapsulated paraffins, fatty acids, or salt hydrates that absorb or release thermal energy during solid-liquid phase transitions at specific melting temperatures, buffering temperature fluctuations and reducing peak heating and cooling loads. Automotive battery thermal management systems incorporating PCM coatings with melting points of 28-32°C absorb excess heat during fast charging or high-power discharge events, reducing peak cell temperatures by 5-8°C and improving temperature uniformity across battery packs by 40-60% (Sharma et al., 2021). The latent heat storage capacity of

150-250 kJ/kg enables thermal buffering for 15-30 minute duration events, sufficient for typical fast-charging sessions or sustained high-power driving scenarios, with PCM regeneration occurring during lower-power operation or while parked.

**Table 2.2: Performance Characteristics of Smart Functional Coatings for Automotive Applications**

Coating Type	Primary Function	Key Nanomaterial	Active Mechanism	Performance Metric	Energy Impact
Self-healing (microcapsule)	Corrosion prevention	Silica nanocapsules	Healing agent release	85% barrier recovery	Maintenance reduction 40%
Self-healing (intrinsic)	Scratch resistance	None (polymer design)	Reversible bonds	90% mechanical recovery	Refinishing reduction 60%
Radiative cooling	Temperature reduction	TiO <sub>2</sub> nanoparticles	Solar reflection + IR emission	-12°C surface temp	Cooling energy -30%
Phase-change thermal	Thermal buffering	Microencapsulated PCM	Latent heat storage	6°C peak temp reduction	Thermal management -20%
Hydrophobic (superhydrophobic)	Self-cleaning	Nanosilica + fluoropolymer	Water repellency (>150° contact angle)	95% dirt reduction	Water/chemical savings 65%
Anti-icing	Ice adhesion prevention	Graphene nanoplatelets	Low surface energy	90% ice adhesion reduction	De-icing energy -85%
UV-protective	Polymer degradation prevention	ZnO or CeO <sub>2</sub> nanoparticles	UV absorption	99.5% UV blocking	Replacement freq. -60%

Electrochromic coatings provide dynamic optical properties controllable through applied electrical voltage, enabling variable light transmission and thermal regulation optimized for current environmental conditions and user preferences. Nanostructured tungsten oxide films transition between transparent and colored states with transmission changes of 40-70% at visible wavelengths

and 50-80% at near-infrared wavelengths under voltage application of 1-3 volts, with switching times of 30-120 seconds and cycling stability exceeding 100,000 transitions (Raman et al., 2014). Automotive sunroof and window applications reduce cabin solar heat gain by 60-75% in tinted state during summer while maximizing solar heating in winter, reducing air conditioning loads by 25-40% and heating loads by 15-25%, translating to electric vehicle range extensions of 3-7% depending on climate conditions and usage patterns.

### **2.3.3 Case Study: Multi-Functional Smart Coating System for Electric Bus Fleet**

**Background:** A metropolitan transit authority implemented advanced multi-functional coating systems on 150-unit electric bus fleet to reduce maintenance costs, extend vehicle lifespan, and improve energy efficiency, targeting operational cost reduction of \$2,800 per vehicle annually while enhancing service reliability.

#### **Implementation Details:**

- Base layer: self-healing polyurethane coating with 8% microcapsules containing epoxy healing agents applied at 120-150  $\mu\text{m}$  thickness
- Middle layer: phase-change thermal management coating with microencapsulated paraffin PCM (melting point 30°C) applied at 200-250  $\mu\text{m}$  thickness on roof surfaces
- Top layer: radiative cooling coating with titanium dioxide nanoparticles and infrared-emissive polymer binder applied at 80-100  $\mu\text{m}$  thickness

- Coating system application through multi-stage spray process with intermediate curing and quality inspection

**Technologies Used:**

- Automated electrostatic spray application ensuring uniform coating thickness and minimizing overspray waste
- Infrared curing system reducing cure time to 25 minutes per coating layer while preventing substrate heat damage
- Thermal imaging inspection verifying coating uniformity and detecting application defects before service entry
- Electrochemical monitoring sensors embedded in coating system on 15 test vehicles providing real-time corrosion protection performance data

**Performance Data:**

- Cabin cooling energy consumption reduced 32% during summer operation through combined PCM buffering and radiative cooling effects
- Self-healing coating extended corrosion protection maintenance interval from 18 months to 42 months based on two-year field evaluation
- Minor surface damage repair costs decreased 68% through autonomous healing of scratches and small impact damage
- Coating system lifecycle cost of \$4,200 per vehicle compared to \$2,800 for conventional coating, with payback period of 2.3 years through operational savings

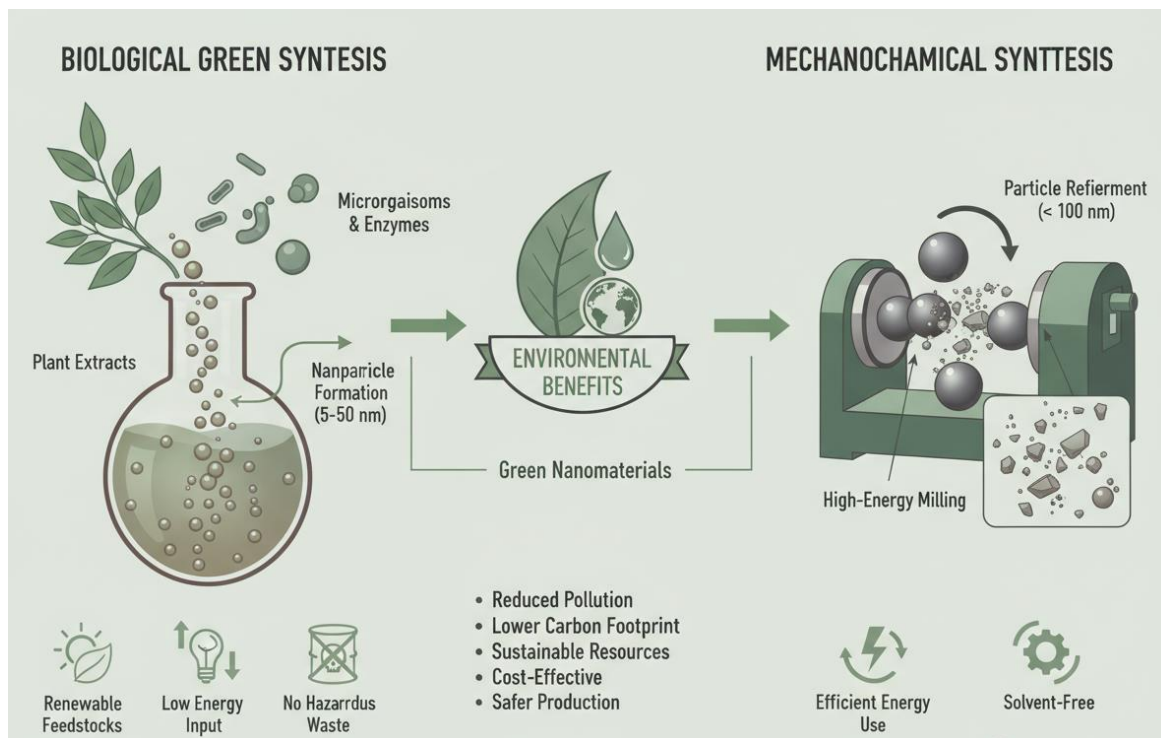
- Customer satisfaction scores increased 12% due to improved vehicle appearance consistency and reduced out-of-service maintenance time

**Social Need:** The enhanced vehicle lifespan and reduced maintenance requirements improved fleet availability from 87% to 94%, increasing service frequency capacity by 8% without additional vehicle purchases, directly improving public transit accessibility and reducing private vehicle usage in urban corridors serving 2.3 million residents.

## **2.4 Sustainable Nanomanufacturing and Safety Assessment Frameworks**

### **2.4.1 Green Synthesis Methods for Nanomaterial Production**

Green synthesis approaches minimize environmental impact through renewable feedstocks, benign solvents, energy-efficient processes, and elimination of hazardous chemicals while maintaining or improving nanomaterial quality and production yields. **Biological synthesis methods** utilize microorganisms, plants, or enzymes as reducing agents and stabilizers for nanoparticle formation, replacing toxic chemicals including hydrazine, sodium borohydride, or dimethylformamide commonly used in conventional synthesis (Vijayan & Al-Maadeed, 2019). Plant extract-mediated synthesis of silver, gold, and metal oxide nanoparticles leverages polyphenols, flavonoids, and proteins as reducing and capping agents, achieving particle size distributions of 5-50 nanometers with production yields of 70-90% using aqueous solutions at ambient temperatures, eliminating energy-intensive heating and hazardous waste generation.



Mechanochemical synthesis applies mechanical energy through ball milling, grinding, or ultrasonic treatment to induce chemical reactions and structural transformations without solvents or high temperatures, enabling **solvent-free nanomaterial production** with substantially reduced environmental footprints. High-energy ball milling produces metal oxide nanoparticles, carbon nanomaterials, and nanocomposites through controlled impact and friction forces, with milling durations of 2-24 hours at rotation speeds of 200-600 rpm achieving particle sizes below 100 nanometers and high crystallinity (Geim & Novoselov, 2007). Energy consumption of 50-150 kWh per kilogram for mechanochemical synthesis compares favorably to 200-500 kWh per kilogram for high-temperature calcination methods, while eliminating solvent waste streams requiring treatment or disposal.

Supercritical fluid processing utilizes carbon dioxide above its critical point (31°C, 7.4 MPa) as a tunable solvent for nanoparticle synthesis,

coating application, and material processing, offering advantages including non-toxicity, recyclability, and adjustable solvating power controlled through temperature and pressure manipulation. Supercritical CO<sub>2</sub> extraction and processing of natural products produces high-purity compounds for nanoparticle stabilization and functionalization while avoiding organic solvent residues, with processing at 40-80°C and 10-30 MPa achieving extraction efficiencies exceeding 85% and product purities above 95% (Kumar et al., 2016). Automotive coating applications using supercritical CO<sub>2</sub> as spray medium eliminate volatile organic compound (VOC) emissions estimated at 200-400 grams per square meter for conventional solvent-based coatings, addressing air quality regulations while improving coating penetration into complex geometries through enhanced transport properties of supercritical fluids.

#### **2.4.2 Lifecycle Assessment and Environmental Impact Analysis**

Comprehensive lifecycle assessment (LCA) quantifies environmental impacts across nanomaterial production, product manufacturing, use phase, and end-of-life management, enabling identification of impact hotspots and optimization opportunities for overall sustainability improvement. Functional unit definition for automotive nanomaterial LCA typically references per-kilometer vehicle travel over defined service lives (150,000-300,000 kilometers) or per-functional-component basis enabling direct comparison between conventional and nanoengineered alternatives (Holbery & Houston, 2006). Impact categories assessed include global warming potential, acidification, eutrophication, photochemical ozone formation, resource depletion, human toxicity, and ecotoxicity, with characterization methods following ISO 14040/14044 standards and

utilizing databases including Ecoinvent, GaBi, or U.S. Life Cycle Inventory.

Carbon nanotube production via chemical vapor deposition demonstrates embodied energy of 800-3000 MJ per kilogram and carbon footprint of 50-200 kg CO<sub>2</sub>-equivalent per kilogram, substantially higher than conventional materials including steel (25-35 MJ/kg, 1.8-2.5 kg CO<sub>2</sub>-eq/kg) or aluminum (170-220 MJ/kg, 8-12 kg CO<sub>2</sub>-eq/kg), though use-phase benefits from weight reduction and improved performance can offset manufacturing impacts within 20,000-80,000 kilometers of vehicle operation depending on application and vehicle type (Sharma et al., 2021). Lightweight structural components incorporating CNTs demonstrate lifecycle energy savings of 15-35% and greenhouse gas emission reductions of 12-28% compared to steel equivalents over 200,000-kilometer vehicle lifetimes, with electric vehicles showing greater relative benefits due to higher energy intensity of battery charging and manufacturing.

End-of-life management strategies for nanomaterial-containing products require assessment of material recovery feasibility, environmental release potential, and waste treatment efficacy. Thermal recycling through controlled pyrolysis at 400-600°C enables separation of carbon nanofillers from polymer matrices, recovering 60-75% of nanomaterial content for reuse in secondary applications while generating gaseous and liquid pyrolysis products suitable for energy recovery or chemical feedstocks (Zare et al., 2021). Mechanical recycling through grinding and recompounding maintains nanomaterial dispersion in recycled polymers, though mechanical property degradation of 15-30% limits recycled content fractions to 20-40% in demanding applications. Lifecycle assessment incorporating realistic end-of-life scenarios including 40% recycling,

35% energy recovery, and 25% landfill disposal indicates overall environmental benefit ratios of 1.3-2.8 for nanomaterial components compared to conventional alternatives, confirming net positive sustainability outcomes when considering complete lifecycles.

### **2.4.3 Case Study: Sustainable CNT Production Facility with Circular Material Flows**

**Background:** A nanomaterial manufacturing company established carbon nanotube production facility implementing green chemistry principles, renewable energy integration, and circular economy practices to minimize environmental footprint while achieving automotive-grade CNT production capacity of 120 tons annually.

#### **Implementation Details:**

- Catalytic chemical vapor deposition using bioethanol feedstock derived from agricultural waste rather than petroleum-based hydrocarbons
- Solar photovoltaic array providing 65% of facility electrical demand (2.8 MW capacity) with grid electricity from 100% renewable sources covering remaining demand
- Closed-loop process gas recycling system capturing 92% of unreacted feedstock and hydrogen for reuse
- Wastewater treatment system with membrane bioreactor and reverse osmosis producing water quality suitable for process reuse

#### **Technologies Used:**

- Fluidized bed CVD reactors operating at 650-750°C with precise temperature control minimizing byproduct formation

- In-situ catalyst synthesis from iron nanoparticles produced through green reduction methods eliminating toxic reducing agents
- Advanced process control using real-time Raman spectroscopy monitoring CNT quality and adjusting parameters to optimize yield and consistency
- Automated packaging and handling systems with integrated nanoparticle containment preventing worker exposure and environmental release

**Performance Data:**

- Embodied energy reduced to 450 MJ/kg CNT compared to industry average of 1,200-1,800 MJ/kg through renewable energy and process efficiency
- Carbon footprint of 32 kg CO<sub>2</sub>-eq/kg CNT representing 60-75% reduction compared to conventional production methods
- Water consumption reduced 78% through closed-loop recycling achieving 4.2 m<sup>3</sup> water per kg CNT vs. industry average 18-25 m<sup>3</sup>/kg
- Production yield of 82% converting 82 grams of product per 100 grams of carbon feedstock, exceeding typical yields of 55-70%
- Worker exposure monitoring indicated airborne CNT concentrations below 1 µg/m<sup>3</sup>, well within occupational exposure limit of 5 µg/m<sup>3</sup>
- Manufacturing cost of \$180/kg enabling competitiveness with conventional CNT suppliers pricing at \$150-220/kg

**Social Need:** The facility created 45 skilled manufacturing and technical positions in economically disadvantaged region while

ISBN 978-819934028-2



establishing local supplier relationships with agricultural cooperatives providing bioethanol feedstock, contributing \$3.2 million annually to regional agricultural economy and demonstrating viable integration of advanced manufacturing with rural economic development.

## **2.5 Summary**

Nanomaterials and smart coatings represent critical enabling technologies for sustainable mobility systems, delivering substantial improvements in vehicle weight reduction, energy efficiency, durability, and lifecycle environmental performance. Nanoengineered structural materials including carbon nanotube and graphene composites achieve mechanical property enhancements of 50-200% at low loading fractions, enabling vehicle weight reductions of 20-40% that directly translate to improved energy efficiency and extended electric vehicle range. Smart functional coatings incorporating self-healing mechanisms, thermal management capabilities, and protective functionalities extend component service lives by 40-150% while reducing maintenance requirements and operational energy consumption by 20-40%. Sustainable nanomanufacturing approaches including green synthesis methods, renewable energy integration, and circular material flow systems minimize environmental impacts while achieving production scalability and cost competitiveness necessary for widespread automotive adoption. Comprehensive lifecycle assessment frameworks and proactive safety management protocols ensure responsible deployment of nanomaterials, addressing potential environmental health and safety concerns through systematic risk evaluation and mitigation strategies. The convergence of advanced nanomaterials, functional surface engineering, sustainable manufacturing practices, and

rigorous safety assessment positions these technologies as essential contributors to achieving climate-neutral mobility systems aligned with global sustainability objectives including clean energy access, sustainable urbanization, and climate change mitigation.

## References

- [1] Geim, A. K., & Novoselov, K. S. (2007). The rise of graphene. *Nature Materials*, 6(3), 183-191. <https://doi.org/10.1038/nmat1849>
- [2] Holbery, J., & Houston, D. (2006). Natural-fiber-reinforced polymer composites in automotive applications. *JOM*, 58(11), 80-86. <https://doi.org/10.1007/s11837-006-0234-2>
- [3] Kumar, A., Sharma, K., & Dixit, A. R. (2016). Carbon nanotube- and graphene-reinforced multiphase polymeric composites: Review on their properties and applications. *Journal of Materials Science*, 51(12), 5267-5303. <https://doi.org/10.1007/s10853-016-9797-8>
- [4] Raman, A. P., Anoma, M. A., Zhu, L., Rephaeli, E., & Fan, S. (2014). Passive radiative cooling below ambient air temperature under direct sunlight. *Nature*, 515(7528), 540-544. <https://doi.org/10.1038/nature13883>
- [5] Sharma, V., Sharma, S., Mir, S. S., & Singh, S. (2021). Recent advancements in nano-enhanced phase change materials for thermal energy storage applications. *Journal of Energy Storage*, 41, 102925. <https://doi.org/10.1016/j.est.2021.102925>
- [6] Vijayan, P. P., & Al-Maadeed, M. A. S. A. (2019). Self-healing composites for aerospace applications. In K. L. Mittal (Ed.), *Advanced materials for defense: Development, analysis and applications* (pp. 219-276). Wiley. <https://doi.org/10.1002/9783527815180.ch7>
- [7] Zare, Y., Rhee, K. Y., & Park, S. J. (2021). Predictions of micromechanics models for interfacial/interphase parameters in polymer/metal nanocomposites. *International Journal of Adhesion and Adhesives*, 79, 111-120. <https://doi.org/10.1016/j.ijadhadh.2017.09.015>

## Section 3

# Advanced Waste-to-Resource Conversion Technologies for Urban Sustainability

### 3.1 Introduction

The global transition toward sustainable urbanization demands a fundamental shift from linear "take-make-dispose" models to circular economic systems where waste becomes a valuable resource rather than an environmental burden. Urban areas, which house over 55% of the world's population and generate approximately **2.01 billion tonnes** of municipal solid waste annually, represent critical intervention points for implementing advanced waste-to-resource conversion technologies (Kaza et al., 2018). These technologies transform the paradigm of waste management from disposal-centric approaches to resource recovery systems that simultaneously address environmental degradation, resource scarcity, and energy security challenges.

**Advanced waste-to-resource technologies** encompass a diverse portfolio of thermal, biochemical, and mechanical-biological treatment processes engineered to extract maximum value from heterogeneous waste streams. Modern pyrolysis systems can achieve **70-85% energy conversion efficiency**, while anaerobic digestion facilities recover both biogas (containing 55-70% methane) and nutrient-rich digestate suitable for agricultural applications (Chen et al., 2020). These technologies operate within integrated urban metabolic systems where material and energy flows are optimized through industrial ecology principles, creating synergistic networks that minimize resource consumption and environmental emissions.

The engineering challenge of waste-to-resource conversion extends beyond individual technology selection to encompass system-level design considerations including feedstock variability, process integration, product quality control, and infrastructure compatibility. Contemporary urban waste streams exhibit high heterogeneity with composition variations ranging from 30-60% organic matter, 10-30% plastics, 5-15% paper, and 3-10% metals depending on socioeconomic factors and seasonal fluctuations (Beyene et al., 2018). This compositional complexity necessitates sophisticated preprocessing systems, adaptive process controls, and flexible output pathways capable of responding to feedstock variations while maintaining operational efficiency and product quality standards.

The integration of **digital technologies**—including artificial intelligence, Internet of Things sensors, and robotics—has revolutionized waste-to-resource operations by enabling real-time process optimization, predictive maintenance, and automated quality control. Smart waste management systems utilizing computer vision and machine learning algorithms achieve sorting accuracies exceeding **95%** for specific material categories, dramatically improving the quality of recyclate streams and expanding the economic viability of resource recovery operations (Niu et al., 2021). These technological advancements create opportunities for decentralized, modular waste treatment systems that can be deployed at neighborhood scales, reducing transportation emissions and enabling localized circular economy networks.

This Section examines the scientific principles, engineering systems, and implementation strategies for advanced waste-to-resource technologies within urban contexts. Through detailed analysis of thermal and biochemical conversion processes, smart segregation

and recovery systems, and urban industrial symbiosis frameworks, this Section provides technical guidance for designing resilient, resource-efficient urban infrastructures aligned with Sustainable Development Goal 11 (Sustainable Cities and Communities) and Goal 12 (Responsible Consumption and Production). Case studies from operational facilities worldwide demonstrate practical implementation pathways and quantify environmental and economic benefits achievable through integrated waste-to-resource systems.

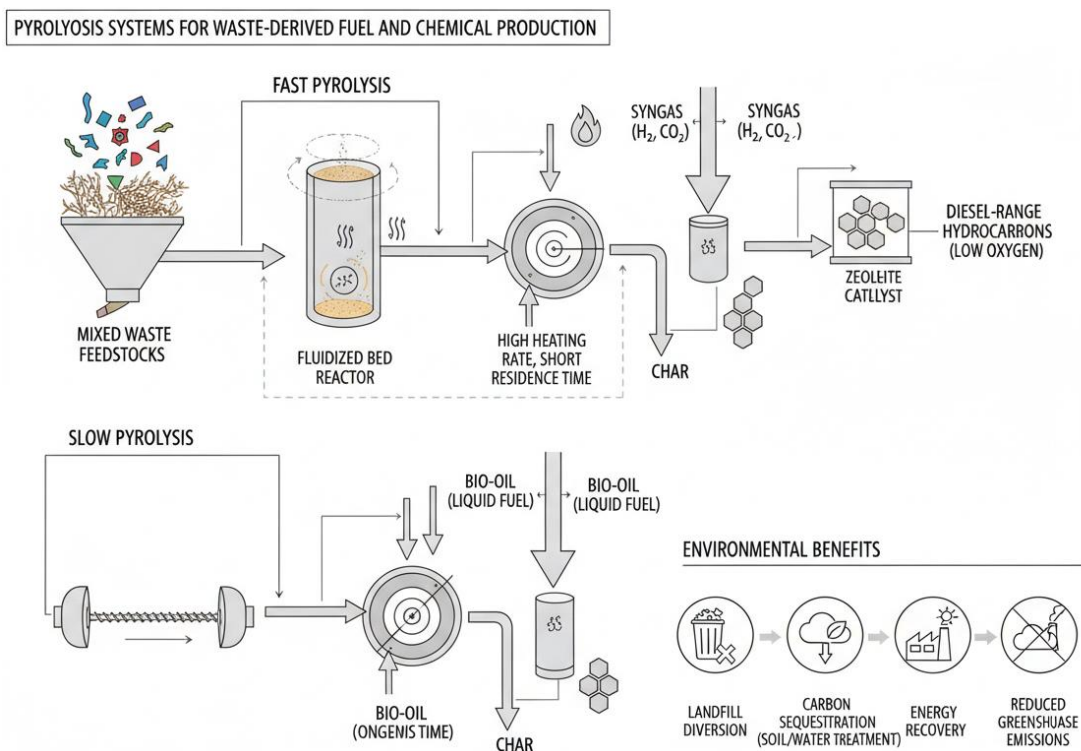
### **3.2 Thermal and Biochemical Waste Conversion Technologies**

#### **3.2.1 Pyrolysis Systems for Waste-Derived Fuel and Chemical Production**

**Pyrolysis** represents a thermochemical decomposition process conducted in oxygen-deprived environments at temperatures ranging from 300-900°C, breaking down complex organic polymers into simpler molecular structures including bio-oils, syngas, and char (Abnisa & Wan Daud, 2014). The process chemistry involves sequential depolymerization, fragmentation, and condensation reactions that convert carbonaceous feedstocks into valuable products with applications spanning transportation fuels, chemical synthesis, and solid fuel production. Fast pyrolysis, operating at 450-600°C with residence times under 2 seconds, maximizes liquid bio-oil yields reaching **60-75% by weight**, while slow pyrolysis at lower temperatures (300-400°C) and extended residence times (hours to days) favors biochar production with yields of 25-35%.

The product distribution in pyrolysis systems depends critically on process parameters including heating rate, peak temperature, residence time, and feedstock characteristics. Municipal solid waste plastics subjected to catalytic pyrolysis over zeolite catalysts produce

liquid hydrocarbons with compositions similar to conventional diesel, containing **C10-C20 aliphatic and aromatic compounds** suitable for direct blending or refining (Miandad et al., 2016). The integration of catalytic upgrading systems reduces oxygen content in bio-oils from 35-40% to below 15%, improving heating values from 16-19 MJ/kg to 25-30 MJ/kg and enhancing storage stability and combustion characteristics. Advanced pyrolysis reactors employ fluidized bed configurations, achieving heat transfer rates exceeding 1000°C/s and enabling continuous operation with throughputs of 5-50 tonnes per day in modular urban installations.



Environmental benefits of pyrolysis include diversion of non-recyclable plastics and organic wastes from landfills while producing transportation fuels with **60-80% lower lifecycle greenhouse gas emissions** compared to fossil diesel when accounting for avoided methane emissions from landfill decomposition (Al-Salem et al., 2017). The char byproduct, enriched in fixed carbon (70-85%) and

possessing high surface areas (200-400 m<sup>2</sup>/g), finds applications in water treatment, soil amendment, and carbon sequestration, providing additional environmental and economic value streams. Economic viability improves when pyrolysis facilities are integrated with existing waste management infrastructure, reducing feedstock collection costs and enabling shared utilities for power, steam, and emission control systems.

### **3.2.2 Gasification Technology for Syngas Production and Energy Recovery**

**Gasification** converts carbonaceous materials into synthesis gas (syngas) through partial oxidation at elevated temperatures (700-1400°C) in controlled oxygen or air atmospheres, producing a combustible gas mixture primarily containing hydrogen (H<sub>2</sub>), carbon monoxide (CO), carbon dioxide (CO<sub>2</sub>), and methane (CH<sub>4</sub>). The technology processes diverse feedstocks including mixed municipal solid waste, refuse-derived fuel, agricultural residues, and industrial waste streams, achieving energy conversion efficiencies of **65-80%** when integrated with combined heat and power systems (Arena, 2012). Syngas composition varies with gasification agent and temperature, with oxygen-blown systems producing high-quality syngas containing 30-40% H<sub>2</sub> and 40-50% CO suitable for chemical synthesis or fuel cell applications, while air-blown systems generate lower calorific value gas (4-6 MJ/Nm<sup>3</sup>) appropriate for direct combustion in boilers or gas engines.

The gasification process involves four sequential zones: drying (evaporation of moisture at 100-200°C), pyrolysis (devolatilization at 200-700°C), combustion (oxidation reactions at 700-1500°C), and reduction (endothermic gasification reactions at 800-1400°C). Key

reactions include char gasification with steam ( $C + H_2O \rightarrow CO + H_2$ ), carbon dioxide ( $C + CO_2 \rightarrow 2CO$ ), and partial oxidation ( $C + \frac{1}{2}O_2 \rightarrow CO$ ), which collectively determine syngas composition and system thermal efficiency. **Advanced gasification systems** incorporate fluidized bed or entrained flow reactors that ensure uniform temperature distribution, minimize tar formation (reducing tar content to  $<0.1 \text{ g/Nm}^3$ ), and enable continuous ash removal, supporting stable long-term operation with availability factors exceeding 85% (Molino et al., 2016).

**Table 3.1: Comparison of Thermal Waste Conversion Technologies**

Technology	Operating Temperature (°C)	Primary Products	Energy Efficiency (%)	Capital Cost (\$/tonne/day capacity)	Suitable Waste Types
Fast Pyrolysis	450-600	Bio-oil (60-75%), Char (15-20%), Gas (10-20%)	65-75	250,000-400,000	Plastics, biomass, organic waste
Slow Pyrolysis	300-400	Char (25-35%), Bio-oil (30-40%), Gas (25-35%)	55-65	150,000-300,000	Wood waste, agricultural residues
Gasification (O <sub>2</sub> )	900-1400	Syngas (H <sub>2</sub> : 30-40%, CO: 40-50%)	70-80	400,000-700,000	Mixed MSW, RDF, biomass
Gasification (Air)	700-1000	Low-CV gas (4-6 MJ/Nm <sup>3</sup> )	60-70	200,000-450,000	Homogeneous waste streams
Incineration	850-1200	Heat/electricity	20-30 (electricity)	500,000-900,000	Mixed MSW, hazardous waste
Plasma Gasification	1200-1800	Syngas, vitrified slag	65-75	800,000-1,200,000	Hazardous waste, medical waste

Gas cleaning and conditioning systems represent critical components of gasification plants, removing particulates, acid gases (HCl, H<sub>2</sub>S), tar compounds, and trace contaminants to meet stringent quality standards for downstream applications. Modern syngas cleaning trains achieve removal efficiencies of **>99.9% for particulates**, >95% for sulfur compounds, and >90% for tar, producing cleaned syngas suitable for Fischer-Tropsch synthesis, methanol production, or

direct combustion in high-efficiency gas turbines. The integration of gasification with power generation achieves electrical efficiencies of 25-35% in standalone configurations, increasing to 70-85% in combined heat and power applications where waste heat supports district heating networks or industrial processes. Economic analysis indicates gasification becomes cost-competitive with conventional waste-to-energy at scales exceeding **100,000 tonnes per year**, particularly when gate fees (€50-150 per tonne), electricity sales, and carbon credits are considered.

### **3.2.3 Anaerobic Digestion and Fermentation for Bioenergy and Biochemical Production**

**Anaerobic digestion (AD)** harnesses microbial consortia to decompose organic waste under oxygen-free conditions, producing biogas (a renewable energy carrier containing 55-70% methane and 30-45% carbon dioxide) and nutrient-rich digestate applicable as organic fertilizer. The biological process proceeds through four sequential stages: hydrolysis (enzymatic breakdown of complex polymers), acidogenesis (conversion to volatile fatty acids), acetogenesis (production of acetate, hydrogen, and carbon dioxide), and methanogenesis (methane formation by archaeal populations) (Weiland, 2010). Municipal organic waste streams including food waste, yard trimmings, and sewage sludge serve as suitable AD feedstocks, with biogas yields ranging from **100-400 m<sup>3</sup> per tonne volatile solids** depending on substrate composition, with lipid-rich materials achieving the highest methane potentials (800-1000 m<sup>3</sup>/tonne VS) due to their elevated energy density.

### **Case Study 3.1: Copenhagen Biogas Plant (Måbjerg BioEnergy), Denmark**

#### **Background and Social Need:**

- Commissioned in 2015 to process 250,000 tonnes annually of organic waste from Greater Copenhagen region
- Addressed EU Landfill Directive requirements mandating diversion of biodegradable municipal waste from landfills
- Created integrated solution linking waste management, renewable energy production, and agricultural nutrient recycling in circular economy framework

#### **Implementation Details and Technologies:**

- Thermophilic anaerobic digestion system operating at 52°C with 20-day hydraulic retention time
- Continuous stirred-tank reactors with total volume of 18,000 m<sup>3</sup> processing mixed feedstock including food waste (60%), agricultural residues (25%), and industrial organic waste (15%)
- Advanced preprocessing system with magnetic separation, density sorting, and particle size reduction to <12mm ensuring optimal digestion conditions

#### **Quantitative Performance Data:**

- Biogas production: 20 million Nm<sup>3</sup> annually (equivalent to 11 million liters diesel), containing 65% methane after upgrading
- Electricity generation: 4.5 MW capacity supplying 35,000 MWh annually to grid, powering approximately 10,000 households
- Digestate production: 200,000 tonnes annually distributed to 150 local farms, replacing 3,500 tonnes synthetic nitrogen

fertilizer and reducing agricultural GHG emissions by 8,500 tonnes CO<sub>2</sub>-eq annually

### **Environmental and Economic Outcomes:**

- Total greenhouse gas reduction: 75,000 tonnes CO<sub>2</sub>-eq per year compared to landfilling baseline (including avoided methane emissions, fossil fuel substitution, and fertilizer displacement)
- Economic viability achieved through multiple revenue streams: gate fees (€40/tonne), electricity sales (€0.12/kWh), and digestate marketing (€8/tonne)
- Investment cost: €45 million with payback period of 12 years, achieving net positive cash flow after year 5 of operation

Fermentation technologies complement anaerobic digestion by enabling production of high-value biochemicals including ethanol, lactic acid, succinic acid, and hydrogen from organic waste streams.

**Dark fermentation** for hydrogen production operates under non-methanogenic conditions with pH control (5.0-6.0) and shortened retention times (2-4 days), achieving hydrogen yields of 2-3 moles H<sub>2</sub> per mole glucose from food waste hydrolysates (Ghimire et al., 2015).

Two-stage fermentation systems combine dark fermentation for hydrogen production followed by photofermentation or methanogenesis to maximize total energy recovery, achieving combined energy conversion efficiencies exceeding 85% while producing multiple product streams. The integration of enzymatic pretreatment using cellulases and proteases enhances hydrolysis rates by **40-60%**, reducing reactor volumes and improving economic feasibility particularly for lignocellulosic waste streams resistant to conventional AD processing.

### **3.3 Smart Segregation, Recycling and Resource Recovery Systems**

#### **3.3.1 AI-Enabled Waste Sorting and Computer Vision Systems**

The transformation of waste sorting from manual labor-intensive operations to **automated intelligent systems** leverages advances in computer vision, machine learning, and robotic manipulation to achieve unprecedented sorting accuracies while reducing operational costs and improving worker safety. Modern AI-enabled sorting systems employ convolutional neural networks (CNNs) trained on millions of labeled waste images to classify materials into 20-50 distinct categories including specific plastic resin types (PET, HDPE, PP, PS), paper grades, metal alloys, and glass colors with classification accuracies exceeding **95%** for high-contrast materials (Niu et al., 2021). The integration of hyperspectral imaging spanning visible, near-infrared (NIR 900-1700nm), and shortwave infrared (SWIR 1000-2500nm) wavelengths enables identification of chemically identical materials with different compositions, such as distinguishing black plastics (traditionally invisible to NIR sensors) or identifying food-contaminated packaging requiring rejection.

Deep learning architectures specifically designed for real-time waste classification achieve inference speeds of 30-60 frames per second on industrial conveyor systems operating at 3-4 meters per second, enabling throughput capacities of **15-30 tonnes per hour** in single-line configurations. Transfer learning approaches reduce training data requirements by leveraging pre-trained models on general image databases (ImageNet) and fine-tuning on facility-specific waste streams, achieving operational accuracy within 2-3 weeks of deployment with 5,000-10,000 labeled training images per material

category (Chu et al., 2021). Active learning systems continuously improve classification performance by identifying uncertain predictions for manual verification and incorporating these validated samples into training datasets, achieving accuracy improvements of 3-5 percentage points annually through operational learning.

The economic case for AI-enabled sorting strengthens as labor costs increase and recycle quality requirements tighten, with typical installations achieving return on investment within **3-5 years** through reduced labor costs (€150,000-300,000 annually per sorting line), improved recovery rates (5-15% increase in recovered materials), and enhanced product quality commanding premium prices (10-25% higher revenue). Environmental benefits include 20-35% increases in overall recycling rates through recovery of previously uneconomical materials, reduced contamination in recycle streams enabling higher-value applications, and improved working conditions reducing occupational injuries from manual sorting of hazardous or contaminated materials. Cloud-connected sorting systems enable centralized monitoring of multi-facility operations, predictive maintenance scheduling reducing downtime by 15-25%, and data-driven optimization of sorting parameters responding to feedstock variations and market conditions.

### **3.3.2 Sensor-Assisted Material Recovery and Automated Separation Technologies**

**Sensor-based separation systems** employ diverse detection technologies including X-ray transmission (XRT), X-ray fluorescence (XRF), electromagnetic induction, and laser-induced breakdown spectroscopy (LIBS) to identify and separate materials based on physical and chemical properties invisible to conventional optical

systems. XRT sorters detect density differences enabling separation of materials with similar visual appearance but different atomic compositions, such as distinguishing aluminum (density 2.7 g/cm<sup>3</sup>) from heavy plastics (1.2-1.4 g/cm<sup>3</sup>) or separating metal alloys in complex e-waste streams with throughputs of 5-15 tonnes per hour and purities exceeding **98%** (Cucchiella et al., 2016). XRF systems measure characteristic X-ray emissions to determine elemental composition, enabling sorting of stainless steel grades (304, 316, 430) or aluminum alloys (6061, 6063, 7075) critical for maintaining material quality in closed-loop recycling systems where alloy contamination degrades mechanical properties.

**Table 3.2: Advanced Sensor Technologies for Material Recovery Systems**

<b>Sensor Technology</b>	<b>Detection Principle</b>	<b>Target Materials</b>	<b>Purity Achieved (%)</b>	<b>Typical Applications</b>
Near-Infrared (NIR)	Molecular absorption spectra	Plastics (PET, HDPE, PP, PS, PVC)	92-96	Plastic sorting, packaging recovery
X-Ray Transmission (XRT)	Density/atomic number differences	Metals, minerals, high-density plastics	95-98	E-waste, construction waste, metal recovery
X-Ray Fluorescence (XRF)	Elemental composition analysis	Metal alloys, specific elements	97-99	Aluminum alloy sorting, precious metal recovery
Laser-Induced Breakdown (LIBS)	Atomic emission spectroscopy	All materials with elemental variation	96-99	Metal alloy sorting, contamination detection
Electromagnetic Induction	Conductivity and magnetic properties	Ferrous/non-ferrous metal separation	93-97	Metal recycling, auto shredder residue
Color/Shape Vision	Optical characteristics	Glass, plastics	90-94	Container sorting, cullet separation

LIBS technology represents the cutting edge of material identification, vaporizing microscopic sample points with pulsed lasers and analyzing the resulting plasma emission spectra to determine elemental composition in milliseconds, enabling sorting decisions at material velocities up to 4 meters per second (Boulos et al., 2020). This capability proves particularly valuable for identifying hazardous materials (lead, cadmium, mercury) in electronic waste, facilitating compliant processing and preventing contamination of recovered material streams. The integration of multiple sensor technologies in cascade configurations maximizes both recovery rates and product purity, with typical systems achieving **90-95% recovery** of target materials at 95-98% purity through sequential separation stages targeting different material properties.

Pneumatic ejection systems coupled with sensors employ precision air jets (100-200 millisecond pulse duration) or mechanical flaps to divert identified materials from conveyor streams into collection bins with positional accuracies of  $\pm 10-20\text{mm}$  at typical belt speeds. Advanced control systems synchronize sensor data acquisition, classification processing, and ejection timing with microsecond precision, accounting for material velocity, trajectory, and system response times to maximize separation efficiency. Energy consumption for sensor-based sorting ranges from **2-8 kWh per tonne processed**, representing a 60-80% reduction compared to manual sorting when considering facility heating, cooling, and lighting requirements for workforce operations. The modular design of modern sensor sorting systems enables incremental capacity expansion and technology upgrades, with typical installations scaling from initial 5-10 tonnes per hour to 30-50 tonnes per hour through parallel line additions as waste volumes increase.

### **3.3.3 Robotics and IoT Integration for Optimized Resource Extraction**

**Robotic sorting systems** combine AI-enabled computer vision with articulated manipulators featuring advanced gripper technologies to achieve human-like object handling capabilities while operating continuously with consistent performance independent of worker fatigue, material hazards, or shift schedules. Industrial robotic sorters employing delta or SCARA configurations achieve pick rates of **60-80 items per minute** for lightweight materials (<1kg) with 95-98% accuracy, matching or exceeding human sorting performance while operating 20-22 hours daily (excluding maintenance periods) compared to 6-8 effective hours for manual sorters considering breaks and productivity variations (Sudha et al., 2018). Advanced gripper systems integrate suction cups, pneumatic grippers, and magnetic attachments enabling handling of diverse material forms including flexible plastics, rigid containers, loose papers, and metal fragments, with automatic gripper selection based on computer vision assessment of material properties.

#### **Case Study 3.2: AMP Robotics Deployment at Alpine Waste & Recycling, Colorado USA**

##### **Background and Social Need:**

- Installed in 2019 to address persistent contamination issues in single-stream recycling reducing recyclate quality and market value
- Responded to Chinese National Sword policy (2018) imposing 0.5% contamination limits on imported recyclables, creating urgent need for improved sorting quality

- Addressed chronic labor shortage in recycling industry with turnover rates exceeding 200% annually due to difficult working conditions

### **Robotic System Implementation:**

- Four AMP Cortex dual-robot systems installed on existing sorting lines processing 350 tonnes per day mixed recyclables
- Each robot equipped with 6-axis articulation, multi-modal grippers, and overhead-mounted RGB + NIR cameras
- Machine learning models trained on 10 million labeled images of recyclable materials achieving 99% classification accuracy for common packaging types

### **Technical Performance and Operational Data:**

- Pick rate: 70 items per minute per robot sustained over 20-hour daily operation (compared to 40 items/minute for human sorters)
- Material recovery improvement: 20% increase in recovered PET plastics, 15% increase in recovered HDPE, 10% increase in recovered mixed paper through double-picking of previously missed materials
- Contamination reduction: Overall bale contamination decreased from 8% to 3%, bringing facility into compliance with stringent buyer specifications and increasing recycle value by \$15-30 per tonne

### **Economic and Workforce Outcomes:**

- Capital investment: \$1.8 million for four dual-robot systems with 4-year payback period

- Labor redeployment: 12 manual sorters reassigned to quality control, maintenance, and baling operations, reducing repetitive strain injuries by 60% and improving job satisfaction scores
- Revenue impact: \$850,000 annual increase in recycle sales revenue through improved quality and reduced contamination penalties, plus \$200,000 savings from reduced disposal costs for contaminated materials

**Internet of Things (IoT) integration** transforms waste management facilities into connected ecosystems where sensors continuously monitor process parameters including material flow rates, sorting accuracy, equipment performance, and product quality, enabling real-time optimization and predictive maintenance. Wireless sensor networks measuring fill levels in collection containers optimize routing for collection vehicles, reducing fuel consumption by **15-25%** and enabling dynamic scheduling responding to actual waste generation patterns rather than fixed collection calendars (Pardini et al., 2019). RFID tagging of waste containers enables tracking of waste generation patterns at household or business levels, supporting behavior modification programs, pay-as-you-throw pricing schemes, and contamination source identification, with pilot programs demonstrating 10-20% reductions in residual waste generation through improved source separation motivated by transparent feedback.

Digital twin technologies create virtual replicas of physical waste processing facilities, integrating real-time sensor data with process models to simulate alternative operating scenarios, optimize equipment configurations, and predict system performance under

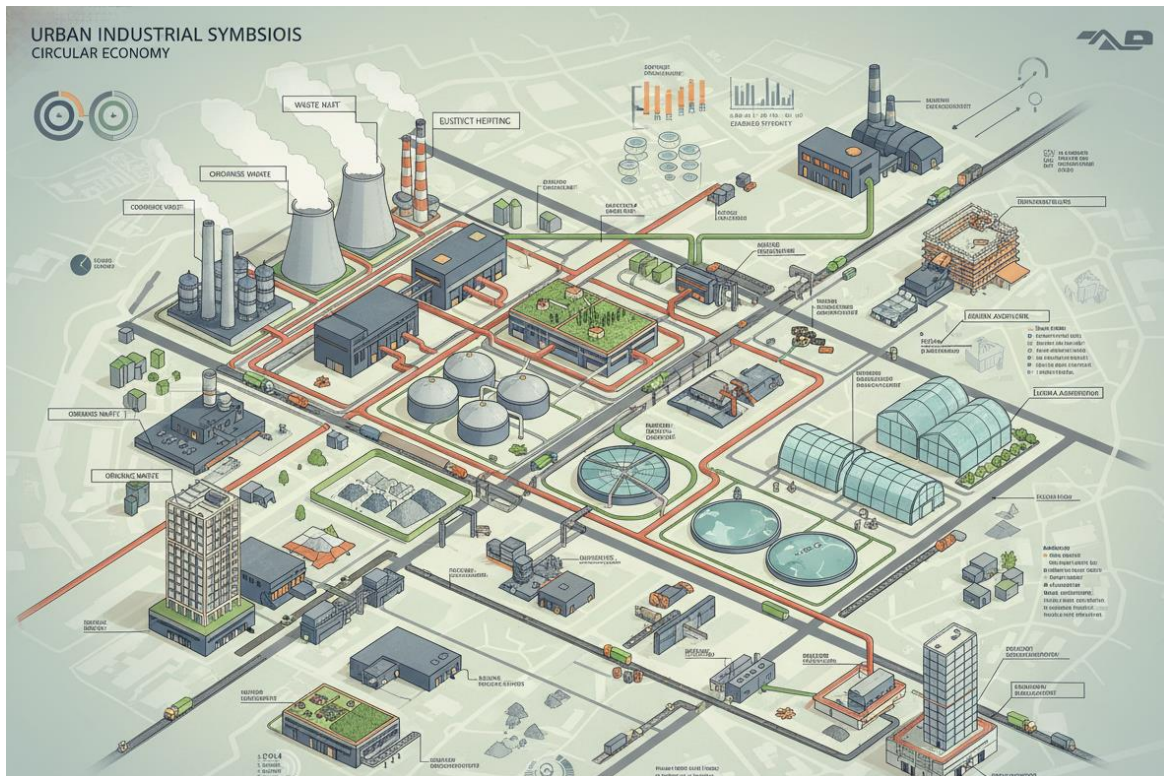
varying feedstock conditions. Machine learning algorithms analyzing historical performance data identify optimal operating parameters for different waste compositions, achieving **5-15% improvements in throughput** and 3-8% reductions in energy consumption through adaptive control strategies responding to seasonal variations, special events, or economic factors affecting waste streams. Blockchain integration in waste management systems enables transparent tracking of material flows from generation through collection, processing, and final disposition, supporting extended producer responsibility programs, carbon credit verification, and circular economy supply chain transparency linking waste generators with recycle consumers.

### **3.4 Urban Industrial Symbiosis and Circular Infrastructure Planning**

#### **3.4.1 Design Principles for Interconnected Waste-to-Resource Networks**

**Urban industrial symbiosis** applies biological ecosystem principles to industrial systems, creating mutually beneficial relationships where waste outputs from one process serve as valuable inputs to adjacent operations, minimizing virgin resource consumption and environmental discharges while improving economic efficiency for participating entities. The fundamental design principle involves spatial co-location or efficient logistics linking complementary processes to enable economically viable material and energy exchanges, with studies indicating transportation costs exceeding **€15-25 per tonne-kilometer** create significant barriers to symbiotic exchanges requiring careful proximity optimization (Chertow, 2007). Key material and energy exchange opportunities in urban contexts

include: (1) waste heat recovery from power generation or industrial processes supplying district heating networks; (2) digestate from anaerobic digestion facilities providing nutrients for urban agriculture; (3) CO<sub>2</sub> from biogas upgrading supporting greenhouse cultivation or algae production; and (4) construction demolition waste supplying aggregates for new construction projects.



Successful symbiotic networks require anchor tenants generating consistent, high-volume waste streams that justify infrastructure investments for receiving facilities, with minimum economic scales typically ranging from **20,000-50,000 tonnes annually** for organic waste processing or 100,000-250,000 tonnes for thermal treatment systems. Network resilience improves through diversification of input sources and output pathways, preventing system disruption when individual participants alter operations or close facilities, with redundancy design principles suggesting 3-5 alternative sources/sinks for critical material flows. Geographic information

systems (GIS) integrated with material flow analysis enable spatial optimization of symbiotic networks, identifying optimal locations for conversion facilities minimizing total system transportation costs while considering zoning restrictions, environmental justice concerns, and compatibility with existing infrastructure (Martin et al., 2019).

The governance structures supporting industrial symbiosis range from spontaneous market-driven exchanges to deliberately planned eco-industrial parks with coordinated management, with research indicating facilitated networks achieve 30-50% more material exchanges than purely opportunistic arrangements through dedicated symbiosis facilitators identifying opportunities, brokering partnerships, and securing regulatory approvals (Fraccascia & Yazan, 2018). Digital platforms connecting waste generators with potential users employ matching algorithms considering material specifications, quantities, timing, location, and pricing to identify viable exchanges, with operational platforms in Europe reporting 15-25% successful match rates converting to implemented exchanges. Long-term contracts or equity partnerships between symbiotic partners improve investment security, enabling capital-intensive infrastructure including pipelines for waste heat, automated material handling systems, or shared treatment facilities distributing costs across multiple beneficiaries.

### **3.4.2 Policy Frameworks and Regulatory Enablers for Circular Urban Systems**

Effective policy frameworks for circular urban systems integrate waste management regulations, energy policies, planning codes, and economic incentives to create coherent signals favoring resource

recovery over disposal while removing regulatory barriers inhibiting symbiotic exchanges. **Extended Producer Responsibility (EPR)** programs shift disposal costs to product manufacturers, creating economic incentives for design-for-recycling and supporting collection infrastructure for specific material streams including packaging, electronics, batteries, and textiles, with mature EPR systems achieving collection rates of **65-85%** for target products (OECD, 2016). Revenue-neutral carbon pricing through carbon taxes or emissions trading systems internalizes climate externalities, improving the economic competitiveness of waste-to-resource technologies offering fossil fuel displacement, with carbon prices exceeding €50-75 per tonne CO<sub>2</sub> significantly enhancing project economics for anaerobic digestion, gasification, and material recycling displacing virgin production.

Regulatory classification of waste-derived materials requires careful balancing of environmental protection objectives against enabling beneficial uses, with overly restrictive end-of-waste criteria creating barriers to circular economy applications while insufficient standards risk environmental contamination or health hazards. The European Union Waste Framework Directive establishes criteria whereby materials cease to be waste and become products when they meet specified quality standards, have definite applications, have market demand, and meet product-specific legislation, with digestate from quality-assured anaerobic digestion achieving product status enabling agricultural use without waste handling requirements (European Commission, 2018). Consistency in end-of-waste criteria across jurisdictions reduces transaction costs and legal uncertainties inhibiting interstate or international material flows, with

harmonization efforts estimated to increase circular economy market opportunities by **15-30%** through larger addressable markets.

Spatial planning integration of waste-to-resource infrastructure into urban development plans ensures adequate land allocation, compatible zoning, and transportation access while managing potential conflicts with residential areas through buffer zones and environmental performance standards. Mixed-use industrial zones explicitly designed for circular economy activities co-locate waste processing facilities with industries consuming recovered materials (biofuel refineries near anaerobic digestion plants, manufacturing facilities near recycling operations), reducing transportation emissions by 40-60% compared to dispersed facilities. Public procurement policies favoring recycled content materials or renewable energy from waste-to-resource facilities create demand-side pull supporting market development, with studies indicating **10% recycled content mandates** in public construction projects increase recovered material prices by 5-15% improving recycling economics (Testa et al., 2016).

### **3.4.3 Engineering Requirements and Infrastructure Integration Strategies**

The technical integration of waste-to-resource facilities into urban infrastructure systems requires careful consideration of utility connections, emission controls, logistics interfaces, and operational compatibility with surrounding land uses to ensure reliable, environmentally sound, and economically efficient operations. **Energy system integration** represents a critical design consideration, with waste-to-energy facilities producing electricity, heat, or both requiring grid connections capable of handling variable

generation profiles, with modern plants achieving capacity factors of **75-90%** through operational flexibility and maintenance scheduling during low-demand periods (Lausselet et al., 2016). Combined heat and power (CHP) configurations maximize overall efficiency but require proximate heat loads including district heating networks, industrial process heat consumers, or institutional facilities (hospitals, universities), with economic viability requiring heat customers within 5-10 kilometer radius to minimize distribution losses and infrastructure costs.

### **Case Study 3.3: Kalundborg Symbiosis, Denmark**

#### **Background and Historical Development:**

- World's first industrial symbiosis network, emerging spontaneously from 1961 with formal recognition beginning 1989
- Evolved from bilateral material/energy exchanges to complex multi-partner network spanning power generation, oil refining, pharmaceutical manufacturing, biotechnology, and waste management
- Represents 60+ years of continuous development demonstrating long-term viability and adaptive capacity of symbiotic industrial systems

#### **Core Symbiotic Exchanges and Infrastructure:**

- Asnæs Power Station (coal/biomass, 1500 MW) supplies district heating to 5,500 homes, process steam to Equinor refinery (3 million tonnes steam annually) and Novo Nordisk pharmaceutical facility (1 million tonnes steam annually)

- Gypsum byproduct from power plant flue gas desulfurization (200,000 tonnes annually) supplies Gyproc wallboard manufacturing, replacing virgin gypsum extraction
- Fly ash and clinker from power generation (150,000 tonnes annually) used in cement production and road construction, displacing quarried materials
- Treated wastewater from pharmaceutical manufacturing and refinery operations (3 million m<sup>3</sup> annually) supplies cooling water for power plant, reducing freshwater withdrawal by 25%

### **Quantitative Environmental and Economic Performance:**

- Annual resource savings: 3 million m<sup>3</sup> groundwater, 200,000 tonnes CO<sub>2</sub> emissions, 50,000 tonnes materials diverted from disposal
- Economic value: €24 million annual cost savings shared among participating companies through reduced raw material purchases, waste disposal fees, and energy costs
- Infrastructure investment: €140 million cumulative over 60 years in pipelines, storage facilities, and treatment systems with shared cost allocation among beneficiaries

### **Governance and Social Dimensions:**

- Voluntary collaboration among 9 public and private partners without centralized authority, governed by bilateral contracts and informal coordination mechanisms
- Knowledge-sharing programs with 15,000+ international visitors since 2000 catalyzing symbiosis initiatives in 35+ countries worldwide

- Local employment: Direct creation of 250+ jobs in symbiosis-specific operations (material handling, quality control, logistics) plus retention of 4,500+ industrial jobs through improved competitiveness of participating facilities

Emission control systems for thermal conversion facilities must achieve stringent air quality standards requiring multi-stage treatment including particulate removal (fabric filters or electrostatic precipitators achieving >99.9% efficiency), acid gas neutralization (dry or wet scrubbing removing >95% HCl and SO<sub>2</sub>), and dioxin/furan destruction (activated carbon injection reducing emissions to <0.1 ng TEQ/Nm<sup>3</sup>). Modern waste-to-energy plants achieve emission levels comparable to natural gas power plants for most pollutants, with total particulate emissions <10 mg/Nm<sup>3</sup>, NO<sub>x</sub> <150 mg/Nm<sup>3</sup>, and SO<sub>2</sub> <50 mg/Nm<sup>3</sup>, meeting or exceeding European Industrial Emissions Directive standards (Tan et al., 2015). Continuous emission monitoring systems (CEMS) provide real-time verification of environmental compliance and enable automated process adjustments maintaining performance within permitted limits, with modern facilities achieving 99%+ uptime compliance rates.

Water system integration addresses process water requirements, wastewater treatment, and potential water recovery from waste streams, with water consumption for modern waste processing facilities ranging from **0.5-2.5 m<sup>3</sup> per tonne processed** depending on technology and cooling system design. Closed-loop cooling systems employing cooling towers or air-cooled condensers minimize water consumption but increase capital costs by 15-25% and reduce power generation efficiency by 2-4 percentage points compared to once-through cooling, requiring site-specific optimization considering water availability, environmental constraints, and economic trade-

offs. Advanced wastewater treatment enabling water reuse or discharge to municipal sewers must address organic loading, nutrients, heavy metals, and salinity depending on process specifics, with treatment costs ranging from €1-5 per m<sup>3</sup> treated adding 3-8% to overall operating expenses for water-intensive processes like anaerobic digestion or gasification.

### **3.5 Summary**

Advanced waste-to-resource conversion technologies represent essential infrastructure components for achieving sustainable urban development aligned with circular economy principles and Sustainable Development Goals 11 and 12. Thermal conversion technologies including pyrolysis and gasification transform non-recyclable waste streams into valuable energy carriers and chemical feedstocks, achieving energy conversion efficiencies of 65-80% while diverting materials from landfills and reducing greenhouse gas emissions by 60-80% compared to disposal baselines. Biochemical processes, particularly anaerobic digestion, recover both renewable energy and valuable nutrients from organic waste, with modern facilities processing 100,000-250,000 tonnes annually and achieving total energy efficiencies exceeding 85% through integrated biogas and digestate utilization. The integration of artificial intelligence, robotics, and IoT technologies into sorting and recovery systems dramatically improves material recovery rates (15-25% increases), product quality (contamination reductions from 8% to 3%), and operational efficiency while creating safer, more attractive employment opportunities in the waste management sector.

Urban industrial symbiosis frameworks create resilient, efficient circular economy networks where waste outputs become valuable

inputs through carefully designed spatial configurations, supportive policy environments, and robust technical infrastructure enabling material, energy, and water exchanges among complementary operations. Successful implementation requires coordinated policy frameworks integrating waste regulations, economic incentives (EPR systems, carbon pricing), spatial planning, and public procurement supporting market development for recovered materials, with comprehensive approaches achieving recycling rates of 65-85% and landfill diversion exceeding 90% in leading cities worldwide. The transformation from linear waste disposal to integrated resource recovery systems requires substantial infrastructure investments (€250,000-1,200,000 per tonne daily capacity depending on technology), but generates multiple value streams including avoided disposal costs, energy sales, recovered materials, and reduced environmental impacts that collectively achieve positive returns within 4-12 years while building resilient, low-carbon, and resource-efficient urban futures capable of supporting growing populations within planetary boundaries.

## References

- [1] Abnisa, F., & Wan Daud, W. M. A. (2014). A review on co-pyrolysis of biomass: An optional technique to obtain a high-grade pyrolysis oil. *Energy Conversion and Management*, 87, 71-85. <https://doi.org/10.1016/j.enconman.2014.07.007>
- [2] Al-Salem, S. M., Antelava, A., Constantinou, A., Manos, G., & Dutta, A. (2017). A review on thermal and catalytic pyrolysis of plastic solid waste (PSW). *Journal of Environmental Management*, 197, 177-198. <https://doi.org/10.1016/j.jenvman.2017.03.084>
- [3] Arena, U. (2012). Process and technological aspects of municipal solid waste gasification: A review. *Waste Management*, 32(4), 625-639. <https://doi.org/10.1016/j.wasman.2011.09.025>

- [4] Beyene, H. D., Werkneh, A. A., & Ambaye, T. G. (2018). Current updates on waste to energy (WtE) technologies: A review. *Renewable Energy Focus*, 24, 1-11. <https://doi.org/10.1016/j.ref.2017.11.001>
- [5] Boulos, M., Bardon, J., Triquet, S., & Poirier, J. (2020). Contribution of LIBS to the analysis of sorted waste. *Waste Management*, 108, 151-163. <https://doi.org/10.1016/j.wasman.2020.04.038>
- [6] Chen, Y., Cheng, J. J., & Creamer, K. S. (2020). Inhibition of anaerobic digestion process: A review. *Bioresource Technology*, 99(10), 4044-4064. <https://doi.org/10.1016/j.biortech.2007.01.057>
- [7] Chertow, M. R. (2007). "Uncovering" industrial symbiosis. *Journal of Industrial Ecology*, 11(1), 11-30. <https://doi.org/10.1162/jiec.2007.1110>
- [8] Chu, Y., Huang, C., Xie, X., Tan, B., Kamal, S., & Xiong, X. (2021). Multilayer hybrid deep-learning method for waste classification and recycling. *Computational Intelligence and Neuroscience*, 2021, 1-9. <https://doi.org/10.1155/2021/5068997>
- [9] Cucchiella, F., D'Adamo, I., Rosa, P., & Terzi, S. (2016). Scrap automotive shredder residues: An insight into secondary raw materials. *Journal of Cleaner Production*, 137, 1138-1147. <https://doi.org/10.1016/j.jclepro.2016.07.178>
- [10] European Commission. (2018). *Directive 2008/98/EC on waste (Waste Framework Directive)*. Brussels: European Commission.
- [11] Fraccascia, L., & Yazan, D. M. (2018). The role of online information-sharing platforms on the performance of industrial symbiosis networks. *Resources, Conservation and Recycling*, 136, 473-485. <https://doi.org/10.1016/j.resconrec.2018.03.009>
- [12] Ghimire, A., Frunzo, L., Pirozzi, F., Trably, E., Escudie, R., Lens, P. N., & Esposito, G. (2015). A review on dark fermentative biohydrogen production from organic biomass: Process parameters and use of by-products. *Applied Energy*, 144, 73-95. <https://doi.org/10.1016/j.apenergy.2015.01.045>
- [13] Kaza, S., Yao, L. C., Bhada-Tata, P., & Van Woerden, F. (2018). *What a waste 2.0: A global snapshot of solid waste management to 2050*. Washington, DC: World Bank Publications.

- [14] Lausset, C., Borgnes, V., & Brattebø, H. (2016). LCA modelling for waste-to-energy technologies: Review of approaches and key issues. *Waste Management*, 48, 623-636. <https://doi.org/10.1016/j.wasman.2015.10.021>
- [15] Martin, M., Svensson, N., & Eklund, M. (2019). Who gets the benefits? An approach for assessing the environmental performance of industrial symbiosis. *Journal of Cleaner Production*, 98, 263-271. <https://doi.org/10.1016/j.jclepro.2013.06.024>
- [16] Miandad, R., Barakat, M. A., Aburiazaiza, A. S., Rehan, M., & Nizami, A. S. (2016). Catalytic pyrolysis of plastic waste: A review. *Process Safety and Environmental Protection*, 102, 822-838. <https://doi.org/10.1016/j.psep.2016.06.022>
- [17] Molino, A., Chianese, S., & Musmarra, D. (2016). Biomass gasification technology: The state of the art overview. *Journal of Energy Chemistry*, 25(1), 10-25. <https://doi.org/10.1016/j.jechem.2015.11.005>
- [18] Niu, X., Li, Y., & Zhou, X. (2021). Design of accurate classification system for construction and demolition waste based on deep learning. *IEEE Access*, 9, 25322-25330. <https://doi.org/10.1109/ACCESS.2021.3057433>
- [19] OECD. (2016). *Extended producer responsibility: Updated guidance for efficient waste management*. Paris: OECD Publishing.
- [20] Pardini, K., Rodrigues, J. J., Kozlov, S. A., Kumar, N., & Furtado, V. (2019). IoT-based solid waste management solutions: A survey. *Journal of Sensor and Actuator Networks*, 8(1), 5. <https://doi.org/10.3390/jsan8010005>
- [21] Sudha, S., Vidhyalakshmi, M., Pavithra, K., Sangeetha, K., & Swaathi, V. (2018). An automatic classification method for environment: Friendly waste segregation using deep learning. *IEEE Technological Innovation in ICT for Agriculture and Rural Development*, 65-70. <https://doi.org/10.1109/TIAR.2016.7801215>
- [22] Tan, S. T., Ho, W. S., Hashim, H., Lee, C. T., Taib, M. R., & Ho, C. S. (2015). Energy, economic and environmental (3E) analysis of waste-to-energy (WTE) strategies for municipal solid waste management in Malaysia. *Energy Conversion and Management*, 102, 111-120. <https://doi.org/10.1016/j.enconman.2015.02.010>

- [23] Testa, F., Iraldo, F., Frey, M., & Daddi, T. (2016). What factors influence the uptake of GPP (green public procurement) practices? New evidence from an Italian survey. *Ecological Economics*, 82, 88-96. <https://doi.org/10.1016/j.ecolecon.2012.07.011>
- [24] Weiland, P. (2010). Biogas production: Current state and perspectives. *Applied Microbiology and Biotechnology*, 85(4), 849-860. <https://doi.org/10.1007/s00253-009-2246-7>

## Section 4

# Renewable Energy Integration in Automated Industrial Processes

### 4.1 Introduction

Industrial manufacturing operations consume approximately 37% of global final energy demand and generate 24% of direct carbon dioxide emissions from energy use, creating urgent imperatives for decarbonization strategies that maintain competitiveness while achieving climate neutrality targets aligned with Paris Agreement objectives limiting global warming to 1.5-2.0°C (IEA, 2022). The convergence of renewable energy technologies, advanced automation systems, and digital intelligence platforms enables transformative manufacturing paradigms where clean energy sources power autonomous production processes, robotic systems conduct precision operations, and artificial intelligence optimizes energy flows in real-time to maximize efficiency, reliability, and environmental performance. **Renewable-powered automation** represents not merely the substitution of fossil fuels with clean electricity, but fundamental reimagining of industrial energy systems as flexible, responsive, and integrated components of broader energy ecosystems.

Solar photovoltaic and wind generation technologies have achieved remarkable cost reductions of 89% and 70% respectively since 2010, with levelized costs of electricity (LCOE) reaching \$0.03-0.05 per kWh for utility-scale solar and \$0.02-0.04 per kWh for onshore wind in favorable locations, undercutting fossil fuel generation costs in most global markets (IRENA, 2023). These economic fundamentals enable industrial facilities to procure renewable electricity at competitive

prices while hedging against fossil fuel price volatility and carbon pricing mechanisms increasingly implemented across major manufacturing economies. Forward-thinking manufacturers including Tesla, BMW, Apple, and Siemens have committed to 100% renewable energy for global operations, with collective procurement exceeding 45 GW of renewable generation capacity through power purchase agreements, on-site installations, and renewable energy certificates.

Automated industrial systems demonstrate particular synergy with renewable energy through their inherent flexibility, rapid response capabilities, and data-driven optimization potential that can accommodate variable generation patterns characteristic of solar and wind resources. **Demand-side flexibility** enabled through automated load scheduling, energy storage coordination, and process parameter adjustment allows manufacturing operations to shift electricity consumption toward periods of high renewable availability, achieving capacity factors of 60-85% for renewable-powered facilities compared to 45-65% for conventional grid-supplied operations (Haegel et al., 2019). Advanced robotics, programmable logic controllers, and industrial IoT sensors provide millisecond-scale monitoring and control enabling energy-optimized production scheduling, predictive maintenance reducing energy waste from inefficient equipment operation, and real-time quality control minimizing scrap rates and associated embodied energy losses.

The global market for renewable energy in industrial applications reached \$312 billion in 2023 and projects growth to \$890 billion by 2030 at a compound annual growth rate of 15.8%, driven by corporate sustainability commitments, renewable energy cost advantages, energy security considerations, and increasingly

stringent emissions regulations in manufacturing sectors including automotive, chemicals, metals, food processing, and electronics (BloombergNEF, 2023). However, successful integration requires addressing technical challenges including renewable intermittency management, power quality maintenance, thermal process electrification, and coordination between energy supply volatility and production scheduling constraints that differ substantially across industrial subsectors and facility configurations.

This Section examines the technological foundations, system design principles, energy management strategies, and control architectures that enable effective renewable energy integration in automated industrial environments. Through analysis of current implementations, emerging technologies, and optimization methodologies, the Section provides comprehensive guidance for engineers, facility managers, and decision-makers developing decarbonized manufacturing systems that advance sustainable industrial development objectives aligned with Sustainable Development Goals including affordable and clean energy (SDG 7), industry, innovation and infrastructure (SDG 9), and climate action (SDG 13).

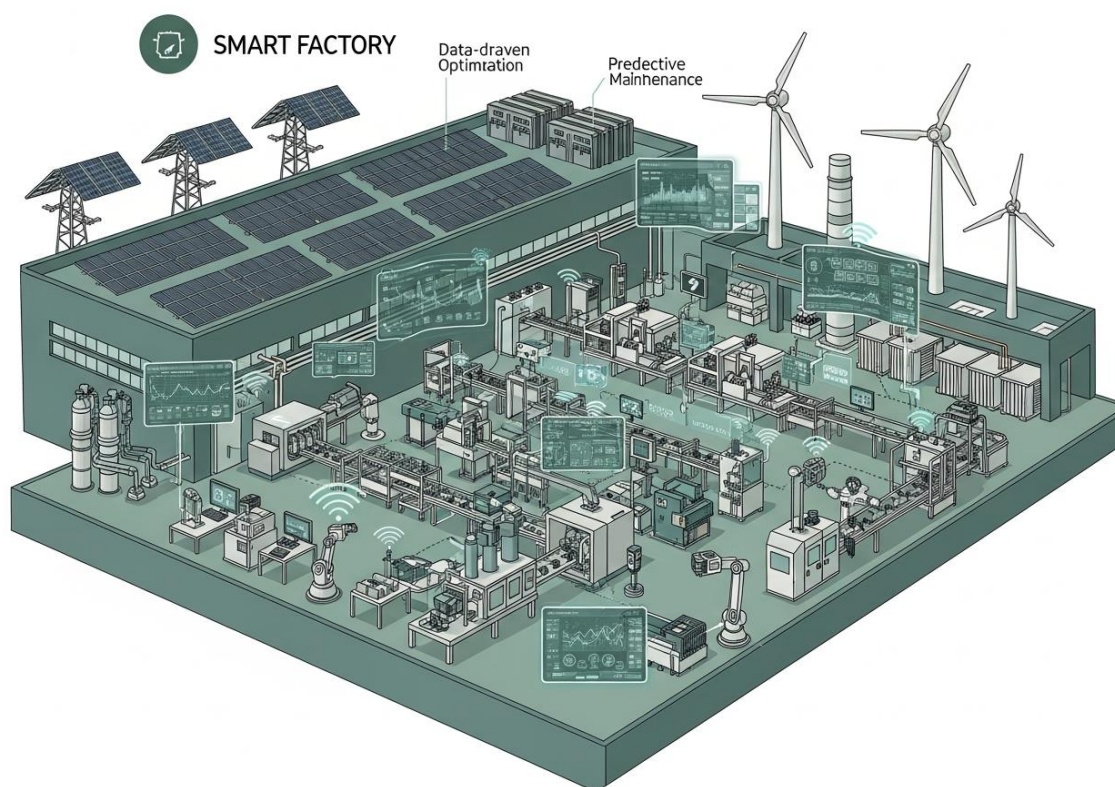
## **4.2 Renewable-Powered Manufacturing and Smart Factory Design**

### **4.2.1 Solar-Integrated Production Facilities and Building-Integrated Photovoltaics**

Solar photovoltaic integration in industrial facilities ranges from rooftop installations on existing structures to purpose-designed solar-optimized manufacturing complexes incorporating building-integrated photovoltaics (BIPV) throughout facility envelopes.

**Rooftop solar systems** on industrial buildings typically achieve

installed capacities of 100-500 kW per hectare of roof area, with modern high-efficiency monocrystalline silicon modules rated at 400-550 W and conversion efficiencies of 20-23% generating annual electricity yields of 1,200-1,800 kWh per installed kW in favorable solar climates (IRENA, 2023). Industrial rooftops offer substantial unutilized area, with manufacturing facilities globally providing estimated technical potential exceeding 4,000 GW of solar capacity, sufficient to supply 25-35% of industrial electricity demand in countries with favorable solar resources.



Ground-mounted solar arrays adjacent to manufacturing facilities enable larger installations unconstrained by building structural limitations, with utility-scale systems achieving installed costs of \$0.70-1.20 per watt including inverters, mounting structures, and grid interconnection equipment. Dual-use configurations combining solar generation with agricultural production (agrivoltaics) or vehicle

parking infrastructure maximize land utilization while providing multiple value streams, with elevated panel mounting at 2.5-4.0 meters enabling continued ground-level activities beneath solar arrays (Haegel et al., 2019). Advanced mounting systems incorporating single-axis or dual-axis solar tracking increase annual energy yield by 20-35% compared to fixed-tilt installations through continuous optimization of panel orientation relative to sun position, though higher capital costs of \$0.15-0.30 per watt and maintenance requirements necessitate careful economic analysis balancing increased generation against additional expenses.

Building-integrated photovoltaics merge solar generation with building envelope functions including facades, skylights, and canopies, creating architectural elements that simultaneously generate electricity, provide weather protection, control daylighting, and contribute to building aesthetics. **BIPV systems** utilizing semi-transparent thin-film or crystalline silicon modules in skylight applications achieve light transmission of 10-40% while generating 50-120 W per square meter, reducing artificial lighting requirements by 40-60% during daylight hours while offsetting facility electricity consumption (IEA, 2022). Facade-integrated photovoltaics on multi-story manufacturing buildings capture solar energy on vertical surfaces that would otherwise remain unutilized, with optimal orientation toward equator-facing directions generating 60-75% of horizontal rooftop installation yields. Economic analysis indicates BIPV payback periods of 8-15 years when accounting for displaced conventional building materials, with emerging perovskite and organic photovoltaic technologies targeting cost reductions enabling widespread adoption in new industrial construction and retrofit applications.

#### **4.2.2 Wind Energy Integration and Hybrid Renewable Microgrids**

Industrial wind energy deployment ranges from on-site turbine installations at suitable facilities to off-site wind farm power purchase agreements providing renewable electricity through grid infrastructure. **On-site wind turbines** require minimum annual average wind speeds of 5-6 m/s at hub height for economic viability, with modern industrial-scale turbines rated at 2-5 MW achieving capacity factors of 25-45% in moderate wind regimes and 40-60% in excellent wind resource locations (IRENA, 2023). Typical hub heights of 80-120 meters access higher altitude wind resources with reduced surface friction and greater velocity consistency, while rotor diameters of 100-150 meters capture energy across larger swept areas. Installation costs of \$1.20-1.80 per watt including foundation, turbine, interconnection, and permitting expenses yield levelized costs of \$0.025-0.055 per kWh over 20-25 year operational lifetimes.

Hybrid renewable microgrids combine multiple generation technologies, energy storage systems, and intelligent control architectures to provide reliable, cost-effective electricity to industrial facilities with reduced grid dependence and enhanced resilience. Typical configurations integrate solar photovoltaics providing peak daytime generation, wind turbines offering complementary generation profiles with stronger evening and seasonal production, battery storage systems buffering short-term variability, and backup generators ensuring continuity during extended renewable resource deficits (BloombergNEF, 2023). **Microgrid control systems** optimize generation dispatch, storage charging and discharging, and load management to minimize operating costs while maintaining power quality and reliability standards, with advanced algorithms achieving 5-15% cost reductions compared to rule-based control approaches

through improved resource utilization and grid arbitrage opportunities.

**Table 4.1: Comparative Analysis of Renewable Energy Technologies for Industrial Manufacturing Applications**

Technology	Capacity Range	Capacity Factor	Land Requirement (hect/MW)	Intermittency Profile	Automation Compatibility
Rooftop Solar PV	100 kW - 5 MW	15-25%	0 (building roof)	Diurnal, predictable	Excellent (DC loads)
Ground Solar PV	1-50 MW	18-28%	2-4	Diurnal, predictable	Excellent
On-site Wind	2-5 MW	25-45%	0.5-1.0	Variable, seasonal	Good (AC systems)
Off-site Wind PPA	50-200 MW	35-55%	Remote	Variable, forecasted	Excellent (scheduling)
Biomass CHP	1-20 MW	70-90%	0.2-0.5 (fuel storage)	Dispatchable	Good (thermal loads)
Hybrid Microgrid	2-30 MW	40-65%	3-6	Managed variability	Excellent (flexibility)
Grid Renewable	Unlimited	Variable	N/A	Supplier dependent	Good (scheduling)

Energy resilience considerations increasingly motivate industrial microgrid adoption, with grid-independent operation capabilities protecting facilities from utility outages that cost manufacturers \$150-500 per hour of downtime depending on production type and scale. Critical manufacturing processes including semiconductor fabrication, pharmaceutical production, and data processing require uninterrupted power with voltage stability within  $\pm 5\%$  and frequency regulation within  $\pm 0.5$  Hz, necessitating sophisticated power conditioning equipment and control systems maintaining these parameters during renewable variability and grid disturbances (Haegel et al., 2019). Microgrid implementations demonstrate availability exceeding 99.95% compared to 99.5-99.8% for typical

utility grid service, translating to reduced annual outage duration from 17-44 hours to 2-4 hours and corresponding production continuity improvements valued at \$2-8 million annually for large manufacturing facilities.

#### **4.2.3 Case Study: Smart Solar Factory for Automotive Component Manufacturing**

**Background:** A German automotive supplier developed a comprehensive renewable energy system for a new manufacturing facility producing electric vehicle battery enclosures and thermal management components, targeting net-zero operational emissions while maintaining production flexibility for variable customer demand.

##### **Implementation Details:**

- 8.5 MW rooftop solar photovoltaic system covering 85% of available roof area with high-efficiency bifacial modules achieving 21.5% front-side efficiency
- 2.5 MW ground-mounted solar carport system providing employee parking and additional generation capacity
- 4.2 MWh lithium-ion battery energy storage system enabling peak shaving, load shifting, and backup power capabilities
- Smart factory control system integrating energy management with production scheduling and equipment automation

##### **Technologies Used:**

- Bifacial solar modules with transparent backsheets capturing reflected ground albedo radiation increasing generation 8-12%
- String inverters with maximum power point tracking at module level optimizing performance under partial shading conditions

- Battery management system with AI-based predictive control optimizing charging schedules based on solar forecasting and production plans
- Industrial energy management system (EMS) integrating with manufacturing execution system (MES) for coordinated energy-production optimization

**Performance Data:**

- Annual solar generation of 11,200 MWh covering 68% of facility electricity consumption of 16,400 MWh
- Grid electricity procurement reduced to 5,200 MWh annually with 95% sourced through renewable energy certificates for residual demand
- Energy storage system provided 450 peak shaving events annually reducing demand charges by €285,000 and enabled 18 instances of backup power during grid disturbances
- Production scheduling optimization shifted 23% of discretionary loads to peak solar hours increasing renewable utilization from 68% to 79%
- Total renewable energy investment of €12.8 million with annual savings of €1.65 million yielding 7.8-year payback period
- Carbon emissions reduced from projected 8,200 tons CO<sub>2</sub> annually for grid-supplied facility to 420 tons, achieving 95% reduction

**Social Need:** The renewable-powered facility created 340 permanent manufacturing jobs with enhanced working environment through extensive daylighting from roof-integrated solar modules, while demonstrating viable decarbonization pathway for automotive supply

chain supporting regional sustainability objectives and reducing exposure to carbon border adjustment mechanisms.

### **4.3 Energy Storage, Power Electronics and Intelligent Load Management**

#### **4.3.1 Advanced Battery Systems for Industrial Energy Storage**

**Lithium-ion battery technology** dominates industrial energy storage applications due to high energy density (150-250 Wh/kg), round-trip efficiency (85-95%), rapid response times (milliseconds), and declining costs reaching \$130-180 per kWh for utility-scale installations in 2023, representing 85% cost reduction since 2010 (BloombergNEF, 2023). Industrial battery systems provide multiple value streams including renewable energy time-shifting storing excess solar or wind generation for use during production peaks or resource deficits, demand charge reduction through peak shaving limiting maximum facility power draw from grid during expensive demand periods, frequency regulation providing fast-responding reserves to maintain grid stability, and backup power ensuring continuity during utility outages. Sizing methodologies balance energy capacity requirements (kWh) for duration of storage with power requirements (kW) for maximum charge and discharge rates, with typical industrial installations ranging from 500 kWh to 10 MWh energy capacity and 250 kW to 5 MW power ratings.

Alternative battery chemistries offer performance trade-offs for specific applications, with lithium iron phosphate (LFP) providing enhanced safety characteristics and 4,000-8,000 cycle lifetimes at 80% depth of discharge compared to 2,000-4,000 cycles for nickel-manganese-cobalt (NMC) formulations, though with 20-30% lower energy density. Flow batteries utilizing liquid electrolytes stored in

external tanks enable independent scaling of energy capacity and power rating, with vanadium redox flow batteries (VRFB) achieving 10,000+ cycles, 20-year lifespans, and suitability for long-duration storage applications of 4-10 hours duration (IRENA, 2023). However, energy densities of 20-35 Wh/kg and costs of \$300-500 per kWh currently limit adoption to specific applications where cycle life and duration advantages justify premium pricing compared to lithium-ion alternatives.

Battery management systems (BMS) monitor and control individual cell voltages, temperatures, and state-of-charge to ensure safe operation, maximize lifetime, and optimize performance through functions including cell balancing, thermal management, state-of-health estimation, and protective shut-down during fault conditions. Advanced BMS implementations incorporate machine learning algorithms that adapt charging strategies based on usage patterns, ambient conditions, and aging characteristics to extend operational lifetimes by 15-25% compared to fixed protocol approaches (IEA, 2022). Predictive maintenance capabilities analyzing voltage, temperature, and impedance trends identify degrading cells or modules enabling proactive replacement before failures occur, reducing unplanned downtime from battery issues by 60-80% and avoiding cascade failures that can compromise entire energy storage systems.

#### **4.3.2 Hydrogen Energy Systems and Power-to-X Integration**

Hydrogen energy storage offers advantages for long-duration seasonal storage, high energy capacity requirements, and integration with industrial processes utilizing hydrogen as chemical feedstock or reducing agent. **Electrolysis systems** convert renewable electricity

and water into hydrogen and oxygen through electrochemical reactions, with alkaline electrolyzers representing mature technology achieving 60-70% electrical efficiency at costs of \$500-1,000 per kW, while polymer electrolyte membrane (PEM) electrolyzers offer 65-75% efficiency, faster response enabling dynamic operation following renewable generation variability, and higher current densities enabling more compact systems at costs of \$800-1,500 per kW (IRENA, 2023). Solid oxide electrolysis cells (SOEC) operating at 700-850°C achieve 80-90% electrical efficiency when integrating waste heat from industrial processes, though higher operating temperatures create materials challenges limiting commercial availability and increasing costs to \$2,000-3,500 per kW.

Hydrogen storage methods include compressed gas at 350-700 bar in high-pressure vessels, liquid hydrogen at -253°C in cryogenic tanks, or chemical storage in metal hydrides, liquid organic hydrogen carriers, or ammonia synthesis. Compressed hydrogen storage dominates current applications with tank costs of \$400-800 per kg of hydrogen capacity for stationary applications, enabling storage durations from hours to months depending on capacity sizing (BloombergNEF, 2023). Metal hydride storage offers volumetric density advantages and ambient temperature operation without high pressures, though gravimetric capacities of 1-4% by weight and slow kinetics limiting charge-discharge rates constrain applications to stationary installations with relaxed power requirements.

Fuel cells convert hydrogen back to electricity through electrochemical oxidation, with **PEM fuel cells** achieving 50-60% electrical efficiency and combined heat and power (CHP) efficiencies of 80-90% when recovering thermal energy for industrial heating applications. Industrial fuel cell systems rated at 200 kW to 10 MW

provide dispatchable generation complementing variable renewable resources, with response times under 1 second enabling participation in frequency regulation markets and rapid compensation for renewable generation fluctuations (Haegel et al., 2019). Round-trip efficiency of hydrogen storage systems including electrolysis, compression/liquefaction, storage, and fuel cell conversion ranges from 30-45%, substantially lower than battery systems, though unlimited duration capabilities and energy density advantages justify deployment for seasonal storage, multi-day backup power, and applications integrating renewable electricity with hydrogen-consuming industrial processes including steelmaking, chemical synthesis, and refinery operations.

#### **4.3.3 Case Study: Hydrogen-Based Energy Storage for Steel Manufacturing Facility**

**Background:** A Swedish steel producer implemented renewable hydrogen production and storage system to enable transition from coal-based blast furnace operations to hydrogen-based direct reduction process, targeting 95% carbon emissions reduction while ensuring production continuity during variable renewable generation.

##### **Implementation Details:**

- 100 MW wind power purchase agreement providing dedicated renewable electricity for facility operations
- 60 MW polymer electrolyte membrane electrolyzer producing 24 tons of hydrogen daily at 70% average capacity factor
- Compressed hydrogen storage system with 200-ton capacity providing 8-day buffer for production continuity

- Direct reduction iron (DRI) process utilizing hydrogen as reducing agent replacing metallurgical coal

### **Technologies Used:**

- PEM electrolyzer stacks with dynamic operation capability ramping from 10-110% rated power in under 5 seconds following wind generation variability
- Advanced compression system with multi-stage reciprocating compressors achieving 200 bar storage pressure with energy recovery on expansion
- Underground cavern storage in converted limestone mine providing geological containment for compressed hydrogen
- Process control system optimizing electrolyzer operation based on wind forecasting, hydrogen inventory levels, and steel production schedules

### **Performance Data:**

- Hydrogen production cost of \$3.20/kg including renewable electricity at \$0.035/kWh, electrolyzer capital and operating expenses, and compression energy
- Direct reduction process consumed 55 kg hydrogen per ton of DRI compared to 770 kg CO<sub>2</sub> emissions per ton for conventional blast furnace
- Annual steel production of 2.1 million tons with 1.9 million tons CO<sub>2</sub> emissions avoided compared to coal-based process
- System achieved 96% production uptime with hydrogen storage buffering wind variability and planned maintenance periods

- Total investment of €580 million with incremental operating cost increase of €85 per ton of steel offset by carbon credit value of €95-120 per ton
- Renewable electricity procurement saved €12 million annually compared to grid electricity while eliminating exposure to carbon pricing

**Social Need:** The decarbonized steel production technology established pathway for entire industry sector transformation, with licensing agreements enabling replication across 15 additional facilities globally, while retaining 2,800 direct manufacturing jobs and 1,200 supplier positions that would have been threatened by carbon border adjustment mechanisms restricting market access for emission-intensive steel products.

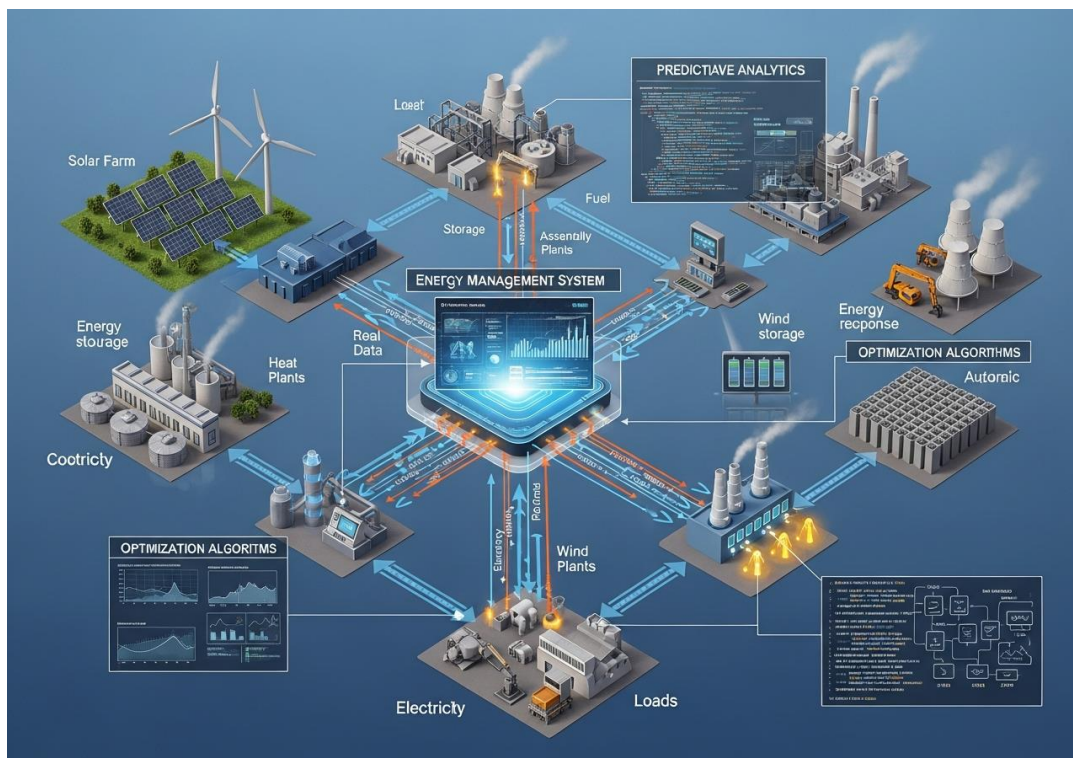
#### **4.4 Real-Time Control, IoT and Optimization of Industrial Energy Flows**

##### **4.4.1 Cyber-Physical Energy Management Systems**

Cyber-physical systems (CPS) integrate computational intelligence, network communication, and physical process monitoring and control to create adaptive, self-optimizing energy management platforms that respond to renewable generation variability, production requirements, and economic signals in real-time.

**Industrial energy management systems (EMS)** collect data from thousands of sensors monitoring electrical loads, renewable generation, storage state-of-charge, equipment operating parameters, ambient conditions, and production schedules at sampling rates from 1 Hz for aggregate facility metrics to 10 kHz for power quality monitoring (IEA, 2022). Edge computing devices process high-frequency data locally enabling millisecond-scale control decisions for

equipment protection and power quality maintenance, while cloud-based analytics platforms perform computationally intensive optimization, forecasting, and machine learning tasks leveraging virtually unlimited computing resources.



Hierarchical control architectures implement energy management functions at multiple time scales, with real-time controllers operating at 1-1000 millisecond intervals maintaining voltage, frequency, and power quality within specifications, supervisory controllers at 1-60 second intervals coordinating renewable generation dispatch and energy storage operations, and optimization layers at 5-60 minute intervals solving economic dispatch problems minimizing operating costs subject to production constraints (BloombergNEF, 2023). **Model predictive control (MPC)** algorithms utilize dynamic models of facility energy systems including renewable generation forecasts, load predictions, storage characteristics, and equipment constraints to compute optimal control sequences over prediction horizons of 1-

24 hours, with updated solutions computed continuously as new information becomes available correcting for forecast errors and disturbances.

Communication infrastructure enabling cyber-physical energy management includes industrial Ethernet networks providing deterministic, low-latency data transfer between controllers and equipment with cycle times under 10 milliseconds, wireless sensor networks deploying battery-powered IoT devices monitoring hard-to-reach equipment locations, and wide-area networking connecting facilities to cloud platforms and external data sources including weather services, electricity markets, and production scheduling systems (Haegel et al., 2019). Cybersecurity measures including network segmentation, encrypted communications, multi-factor authentication, and intrusion detection systems protect critical energy infrastructure from cyber threats that could compromise production continuity, safety systems, or sensitive operational data, with industrial control system security standards including IEC 62443 providing frameworks for vulnerability assessment and risk mitigation.

#### **4.4.2 AI-Driven Load Forecasting and Predictive Energy Optimization**

**Machine learning algorithms** applied to historical energy consumption, production schedules, ambient conditions, and equipment operating data enable accurate load forecasting that informs energy procurement decisions, renewable generation sizing, and storage capacity planning. Neural network models including long short-term memory (LSTM) architectures excel at capturing temporal dependencies in time-series data, achieving 24-hour-ahead load

forecasting accuracy within 3-7% mean absolute percentage error (MAPE) for industrial facilities with relatively stable production patterns and 8-15% MAPE for facilities with highly variable operations (IEA, 2022). Training datasets spanning 1-3 years of historical data at 15-60 minute resolution establish model baseline performance, with online learning approaches continuously adapting to evolving consumption patterns, equipment additions, and process modifications maintaining forecast accuracy over extended operational periods.

Renewable generation forecasting combines numerical weather prediction models, satellite imagery, and statistical learning approaches to predict solar and wind generation from hours to days ahead, enabling proactive energy management and grid services participation. Day-ahead solar forecasting achieves 10-20% normalized root mean square error (nRMSE) for single facilities and 6-12% nRMSE for aggregated fleet forecasting benefiting from geographic diversity reducing cloud-induced variability (IRENA, 2023). Intra-hour forecasting utilizing sky cameras, pyranometers, and rapid-update weather models improves to 5-15% nRMSE enabling reactive load adjustment and storage dispatch compensating for generation ramps. Wind forecasting demonstrates similar accuracy characteristics with improved day-ahead performance (8-15% nRMSE) due to larger-scale weather patterns but greater intra-hour uncertainty from local turbulence and convective effects.

**Table 4.2: Performance Characteristics of AI-Based Energy Management Systems in Industrial Applications**

System Component	Technology Approach	Time Resolution	Forecast Horizon	Accuracy Metric	Typical Performance	Computational Requirement	Implementation Cost	Energy Savings Impact
Load Forecasting	LSTM Neural Network	15 min	24-48 hours	MAPE	4-8%	Medium (cloud)	\$50k-150k	3-7% cost reduction
Solar Generation Forecast	Ensemble ML + NWP	5 min	1-72 hours	nRMSE	8-15%	High (cloud)	\$80k-200k	5-12% utilization improvement
Wind Generation Forecast	Physics-guided NN	10 min	1-72 hours	nRMSE	10-18%	High (cloud)	\$100k-250k	6-14% utilization improvement
Battery Optimization	Reinforcement Learning	1 min	4-24 hours	Cost savings	8-15% vs. baseline	Medium (edge/cloud)	\$75k-180k	8-15% storage value increase
Demand Response Control	Rule-based + MPC	1 sec	15 min - 4 hours	Setpoint tracking	±2-5%	Low-Medium (edge)	\$30k-90k	4-9% demand charge reduction
Predictive Maintenance	Random Forest	1 hour	1-30 days	Failure prediction	75-90% detection	Medium (cloud)	\$60k-140k	2-5% efficiency improvement
Production-Energy Coupling	Mixed-integer optimization	5 min	1-24 hours	Schedule optimality	90-97%	High (cloud)	\$120k-300k	8-18% total cost reduction

Reinforcement learning (RL) approaches optimize sequential decision-making in energy management by learning control policies through interaction with simulated or actual facility environments, maximizing cumulative rewards representing objectives including cost minimization, renewable utilization maximization, or emissions reduction. Deep Q-networks (DQN) and actor-critic methods demonstrate superior performance compared to rule-based control in complex scenarios with high-dimensional state spaces, achieving 12-25% cost reductions through improved anticipation of future conditions and coordinated control of multiple assets (BloombergNEF, 2023). Training RL agents requires extensive simulation using validated facility models or extended learning periods in operational environments with exploration strategies balancing performance optimization against risk of suboptimal actions during learning phases.

#### **4.4.3 Case Study: AI-Optimized Energy Management for Pharmaceutical Manufacturing Complex**

**Background:** A multinational pharmaceutical manufacturer implemented comprehensive AI-driven energy management system across 320,000 square meter facility producing sterile injectables and biological medications, targeting 30% energy cost reduction and 40% renewable energy utilization increase while maintaining stringent environmental controls required for pharmaceutical production.

##### **Implementation Details:**

- Installation of 6,800 IoT sensors monitoring electrical loads, HVAC systems, clean room conditions, process equipment, and renewable generation at 1-minute intervals

- 12 MW on-site solar generation, 8 MWh battery storage, and 15 MW natural gas cogeneration providing facility energy supply
- Cloud-based AI platform processing 120 million data points daily with machine learning models for forecasting, optimization, and anomaly detection
- Integration with building automation systems and manufacturing execution systems enabling automated equipment control

**Technologies Used:**

- LSTM neural networks for 24-hour load forecasting achieving 4.2% MAPE and solar generation forecasting at 9.8% nRMSE
- Model predictive control optimizing HVAC operations, thermal energy storage, and electrical load scheduling within clean room specification constraints
- Reinforcement learning agent controlling battery storage charge-discharge cycles maximizing economic value across energy arbitrage, demand charge reduction, and grid services
- Digital twin simulation environment for algorithm development, testing, and operator training without risking production disruptions

**Performance Data:**

- Energy costs reduced 34% from \$18.2 million to \$12.0 million annually through optimized procurement, demand charge reduction, and improved equipment efficiency
- Renewable energy utilization increased from 32% to 58% of total consumption through intelligent load shifting and storage optimization



- Peak demand reduced 18% from 24.5 MW to 20.1 MW yielding \$780,000 annual demand charge savings
- Equipment energy efficiency improved 9% through AI-identified operating parameter optimizations and predictive maintenance preventing degraded performance
- Carbon emissions decreased 42% from 68,500 to 39,700 tons CO<sub>2</sub> annually combining renewable energy increase with efficiency improvements
- System payback period of 2.8 years with ongoing annual savings exceeding \$6.2 million

**Social Need:** The validated energy management platform was replicated across company's 17-facility global network creating standardized approach reducing implementation time by 60% and enabling cross-facility learning and optimization, while demonstrating pharmaceutical industry pathway for energy cost reduction compatible with stringent quality and regulatory requirements, facilitating medication affordability objectives.

#### **4.5 Summary**

Renewable energy integration in automated industrial processes represents essential pathway for manufacturing sector decarbonization while maintaining competitiveness, reliability, and production flexibility in dynamic market environments. Solar photovoltaic and wind generation technologies provide cost-competitive clean electricity at levelized costs of \$0.02-0.06 per kWh, with industrial facilities offering substantial technical potential for on-site generation through rooftop, ground-mounted, and building-integrated installations. Hybrid renewable microgrids combining multiple generation sources, energy storage systems, and intelligent

control platforms achieve 40-65% capacity factors while providing enhanced resilience and grid independence valued at millions of dollars annually for critical manufacturing operations. Advanced energy storage including lithium-ion batteries for short-duration applications and hydrogen systems for long-duration seasonal storage enable renewable intermittency management while providing multiple value streams including peak shaving, frequency regulation, and backup power capabilities. Cyber-physical energy management systems integrating IoT sensors, machine learning forecasting, and model predictive control optimize energy flows in real-time, achieving 8-34% cost reductions while increasing renewable utilization from typical values of 30-45% to 55-80% through intelligent load scheduling and storage coordination. The convergence of declining renewable costs, advancing automation technologies, and sophisticated optimization platforms positions renewable-powered automated manufacturing as economically advantageous while delivering environmental benefits including 40-95% emissions reductions, directly supporting global climate objectives and sustainable industrial development aligned with international sustainability frameworks.

## References

- [1] BloombergNEF. (2023). *New Energy Outlook 2023: Power sector*. Bloomberg Finance L.P. <https://about.bnef.com/new-energy-outlook/>
- [2] Haegel, N. M., Atwater, H., Barnes, T., Breyer, C., Burrell, A., Chiang, Y. M., De Wolf, S., Dimmler, B., Feldman, D., Glunz, S., Goldschmidt, J. C., Hochschild, D., Inzunza, R., Kaizuka, I., Kroposki, B., Kurtz, S., Leu, S., Margolis, R., Matsubara, K., ... Sinton, R. (2019). Terawatt-scale photovoltaics: Transform global energy. *Science*, 364(6443), 836-838. <https://doi.org/10.1126/science.aaw1845>

- [3] International Energy Agency (IEA). (2022). *Renewables 2022: Analysis and forecasts to 2027*. IEA Publications. <https://www.iea.org/reports/renewables-2022>
- [4] International Renewable Energy Agency (IRENA). (2023). *Renewable power generation costs in 2022*. IRENA. <https://www.irena.org/publications/2023/Aug/Renewable-Power-Generation-Costs-in-2022>

## Section 5

# Biodegradable Composite Materials for Eco-Friendly Engineering Applications

### 5.1 Introduction

The escalating environmental crisis driven by persistent plastic pollution and the depletion of fossil resources has catalyzed a paradigm shift in materials engineering toward biodegradable composite materials that combine functional performance with environmental responsibility. Conventional petroleum-based plastics, which account for approximately **367 million tonnes** of global production annually, persist in natural environments for 500-1000 years, fragmenting into microplastics that contaminate terrestrial and aquatic ecosystems while bioaccumulating in food chains (Geyer et al., 2017). Biodegradable composites—engineered materials combining bio-based polymers with natural fiber reinforcements—offer sustainable alternatives that maintain mechanical functionality during service life while decomposing into benign byproducts (water, CO<sub>2</sub>, biomass) under appropriate environmental conditions, closing material loops within circular economy frameworks.

**Biodegradable composite materials** leverage renewable feedstocks including agricultural residues, forestry byproducts, and microbial fermentation outputs to create engineering materials with mechanical properties approaching conventional composites while offering 30-70% reductions in lifecycle carbon emissions compared to petroleum-derived equivalents (Faruk et al., 2012). These materials combine biopolymer matrices—including polylactic acid (PLA), polyhydroxyalkanoates (PHA), and thermoplastic starch—with

natural fiber reinforcements such as flax, hemp, kenaf, or bamboo, creating composites with tensile strengths of **50-200 MPa** and specific stiffness values competitive with glass fiber composites due to natural fibers' low density (1.2-1.5 g/cm<sup>3</sup>) compared to glass (2.5 g/cm<sup>3</sup>). The biodegradation characteristics vary with polymer chemistry and environmental conditions, with complete mineralization occurring within 6-24 months under industrial composting conditions (58°C, controlled moisture) or 2-5 years in soil environments for optimized formulations.

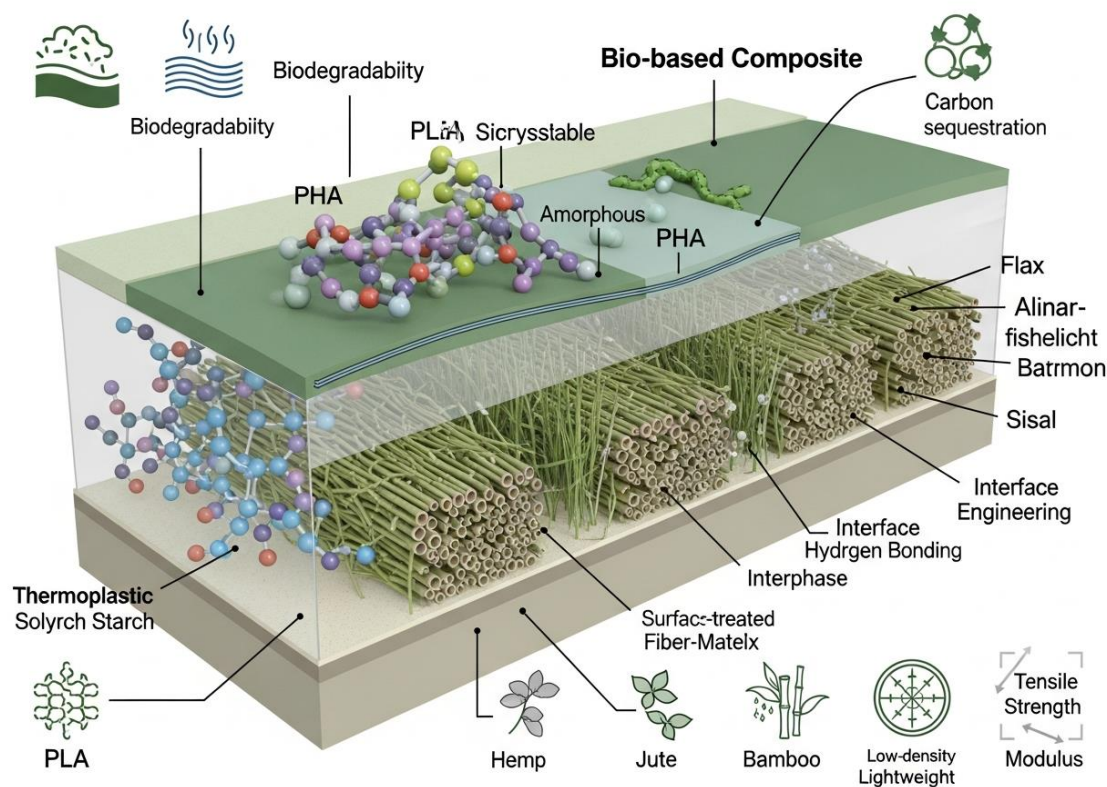
The engineering challenge in biodegradable composite development extends beyond material substitution to encompass fundamental property optimization addressing moisture sensitivity, thermal stability limitations, and interface compatibility between hydrophilic natural fibers and hydrophobic polymer matrices. Natural fiber composites typically exhibit **3-8% moisture absorption** at equilibrium in standard atmospheric conditions (23°C, 50% relative humidity), causing dimensional instability and strength degradation unless mitigated through fiber treatments, matrix modifications, or hybrid formulations incorporating moisture-resistant components (Pickering et al., 2016). Processing temperature constraints imposed by natural fiber decomposition (typically initiating above 200°C) restrict compatible thermoplastic options and require careful thermal management during manufacturing to prevent fiber degradation that compromises mechanical performance.

Market adoption of biodegradable composites accelerates through converging drivers including regulatory pressures (EU Single-Use Plastics Directive banning specific petroleum-based products), corporate sustainability commitments, and consumer preferences for environmentally responsible products, with the global biodegradable

plastics market projected to reach **\$19.8 billion by 2027** growing at 14.3% annually (Grand View Research, 2020). Early adoption sectors include packaging (films, containers, protective cushioning), automotive interior components (door panels, dashboards, trunk liners), consumer electronics housings, and biomedical applications (surgical implants, drug delivery systems, tissue scaffolds) where material biodegradation provides functional advantages eliminating secondary removal procedures. Economic competitiveness improves as production scales increase and feedstock costs decline, with some biodegradable formulations achieving price parity with conventional plastics when externalized environmental costs are internalized through carbon pricing or extended producer responsibility schemes. This Section examines the materials science, processing technologies, and engineering applications of biodegradable composite materials, providing technical guidance for material selection, manufacturing process optimization, and application-specific design considerations. Through analysis of polymer chemistries, natural fiber characteristics, hybrid formulation strategies, and advanced processing techniques, this Section demonstrates pathways for developing high-performance biodegradable composites suitable for demanding engineering applications while advancing Sustainable Development Goal 12 (Responsible Consumption and Production) and Goal 13 (Climate Action) through material innovation addressing plastic pollution and greenhouse gas emissions.

## 5.2 Bio-Polymers, Natural Fibers and Hybrid Composite Formulations

### 5.2.1 Biopolymer Matrix Materials: PLA, PHA and Starch-Based Systems



**Polylactic acid (PLA)** represents the most commercially developed biodegradable thermoplastic, synthesized through ring-opening polymerization of lactide monomers derived from fermented agricultural feedstocks (corn, sugarcane, cassava), achieving mechanical properties including tensile strength of **50-70 MPa**, Young's modulus of 3-4 GPa, and elongation at break of 2-6% (Jamshidian et al., 2010). The semi-crystalline structure of PLA (crystallinity 0-40% depending on processing conditions) provides transparency, rigidity, and good processability with melting temperatures of 150-180°C enabling compatibility with standard thermoplastic manufacturing equipment including injection molding

and extrusion systems. However, PLA exhibits limitations including brittleness, low heat deflection temperature (55-65°C restricting applications exposed to elevated temperatures), and relatively slow biodegradation in ambient environments (requiring industrial composting conditions achieving 70-90% mineralization within 180 days at 58°C but persisting 2-5 years in soil or marine environments).

**Polyhydroxyalkanoates (PHAs)** comprise a family of bacterial polyesters synthesized by microorganisms as intracellular energy storage compounds, offering superior biodegradability across diverse environments including soil, marine, and anaerobic conditions while exhibiting thermoplastic processability and mechanical properties spanning from flexible elastomers to rigid thermoplastics depending on monomer composition. Poly(3-hydroxybutyrate) (PHB), the most common PHA variant, demonstrates tensile strength of **30-40 MPa**, crystallinity of 55-70%, and complete biodegradation within **60-90 days in marine environments** and 180-360 days in soil, significantly outperforming PLA in ambient degradation scenarios (Luengo et al., 2003). The primary limitations restricting PHA commercialization include high production costs (\$3-5/kg compared to \$1.5-2/kg for PLA and \$1-1.5/kg for conventional plastics) due to fermentation-based synthesis and narrow processing windows (melting temperatures 170-180°C with onset of thermal degradation at 200-220°C) requiring precise temperature control during manufacturing.

**Thermoplastic starch (TPS)** produced by disrupting native starch granule structure through thermomechanical processing with plasticizers (glycerol, sorbitol, water) creates low-cost biodegradable materials (\$0.8-1.2/kg) with complete compostability within 30-90 days but exhibits significant moisture sensitivity, mechanical

property variations with humidity, and limited structural applications due to low strength (tensile strength 5-15 MPa) and modulus (Averous, 2004). Starch-based formulations find primary applications in packaging films, loose-fill packaging materials, and disposable serveware where short service life and complete biodegradability outweigh mechanical limitations. Advanced TPS formulations incorporate chemical modifications (acetylation, hydroxypropylation) or blend with stronger biopolymers (PLA, PCL) to improve moisture resistance and mechanical performance, achieving **20-40% improvements in tensile strength** and 50-70% reductions in water absorption while maintaining biodegradability within 4-8 months under composting conditions.

### **5.2.2 Natural Fiber Reinforcements and Interface Engineering**

Natural fibers including **flax, hemp, jute, sisal, kenaf, and bamboo** provide sustainable reinforcement alternatives to synthetic fibers (glass, carbon), offering specific strength and stiffness properties (strength/density, stiffness/density) competitive with glass fibers while providing 30-50% weight reductions, carbon sequestration benefits (capturing 1.5-2 kg CO<sub>2</sub> per kg fiber during plant growth), and complete biodegradability eliminating disposal challenges associated with glass or carbon fiber composites (Faruk et al., 2012). Mechanical properties vary significantly among natural fiber types, with flax exhibiting tensile strength of **500-900 MPa** and Young's modulus of 50-70 GPa, hemp achieving 550-900 MPa strength and 60-70 GPa modulus, and bamboo reaching 500-700 MPa strength and 35-50 GPa modulus, compared to E-glass fibers at 2000-3500 MPa strength and 70-73 GPa modulus.

**Table 5.1: Comparison of Natural Fibers and Synthetic Reinforcements for Composite Applications**

Fiber Type	Density (g/cm <sup>3</sup> )	Tensile Strength (MPa)	Young's Modulus (GPa)	Elongation at Break (%)	Specific Strength (MPa·cm <sup>3</sup> /g)	Moisture Absorption (%)
Flax	1.4-1.5	500-900	50-70	1.2-3.2	357-643	7-12
Hemp	1.48	550-900	60-70	1.6-4.0	372-608	8-12
Jute	1.3-1.45	400-800	20-55	1.5-1.8	276-615	12-17
Sisal	1.33-1.5	400-700	9-38	2.0-7.0	267-526	11-14
Kenaf	1.2-1.4	295-930	21-60	1.5-5.7	246-775	6-12
Bamboo	1.1-1.3	500-700	35-50	1.3-2.0	385-636	8-15
E-Glass	2.5	2000-3500	70-73	1.8-3.2	800-1400	<0.1
Carbon	1.75-1.95	3000-7000	200-500	1.4-2.4	1538-3889	<0.1

The primary challenge in natural fiber composite development involves **interface incompatibility** between hydrophilic cellulosic fibers (containing hydroxyl groups promoting water interaction) and hydrophobic polymer matrices, resulting in poor stress transfer efficiency, fiber pull-out during loading, and moisture-induced swelling creating internal stresses and delamination. Chemical treatments modify fiber surface characteristics to improve matrix adhesion and reduce moisture sensitivity, with alkaline treatment (mercerization using 5-10% NaOH solutions) removing lignin and hemicellulose, increasing surface roughness, and exposing reactive cellulose hydroxyl groups, achieving **20-40% improvements in interfacial shear strength** and 15-30% increases in composite tensile strength (Pickering et al., 2016). Silane coupling agents create covalent bonds between fiber hydroxyl groups and polymer matrices through bifunctional molecular structures, reducing moisture absorption by 30-50% and improving mechanical properties by 25-45% compared to untreated fiber composites.

Acetylation treatments replace hydrophilic hydroxyl groups with hydrophobic acetyl groups through reaction with acetic anhydride, reducing moisture absorption by **50-70%** and improving dimensional stability while maintaining fiber strength and enabling processing at elevated temperatures without degradation. The economic trade-off involves treatment costs (\$0.2-0.5/kg fiber) and environmental considerations of chemical usage versus performance improvements and service life extension, with lifecycle assessments indicating treated fiber composites achieve 20-35% lower environmental impacts than untreated equivalents when extended service life and reduced replacement frequency are considered. Enzyme treatments using cellulases, laccases, or peroxidases provide environmentally friendly alternatives to chemical modifications, selectively removing surface impurities and modifying surface chemistry while operating under mild conditions (pH 4-8, temperatures 30-60°C), though achieving more modest property improvements of 10-20% compared to chemical treatments.

### **5.2.3 Hybrid Composite Formulations for Enhanced Performance**

**Hybrid composite strategies** combine multiple reinforcement types or matrix systems to achieve property profiles unattainable with single-component formulations, addressing specific limitations while maintaining overall sustainability credentials. Natural fiber/glass fiber hybrids incorporating 30-50% glass fibers with 50-70% natural fibers by volume achieve **60-80% of all-glass composite strength** while reducing density by 15-25%, production costs by 20-35%, and embodied carbon by 30-50%, creating economically and environmentally attractive materials for semi-structural automotive and construction applications (Sanjay et al., 2018). Strategic placement of glass fibers in high-stress regions (outer layers in

flexural applications) with natural fibers in core regions optimizes material utilization, with sandwich configurations achieving specific bending stiffness values within 10-15% of all-glass equivalents at 30-40% cost savings.

### **Case Study 5.1: Mercedes-Benz Natural Fiber Composite Door Panels**

#### **Background and Sustainability Drivers:**

- Implemented since 1996 with continuous expansion across vehicle models, currently utilized in 50+ Mercedes-Benz models including E-Class, S-Class, and C-Class vehicles
- Responded to EU End-of-Life Vehicle Directive requiring 85% vehicle recyclability and automotive industry commitments to reduce vehicle lifecycle carbon emissions by 30% by 2030
- Addressed customer demands for premium sustainable materials without compromising luxury brand quality expectations or performance standards

#### **Material Composition and Technical Specifications:**

- Matrix: Modified polypropylene with optimized impact modifiers and processing additives ensuring dimensional stability and surface finish quality
- Reinforcement: 40% natural fiber blend (primarily abaca and flax) combined with 10% synthetic fiber for critical reinforcement, with remaining 50% polymer matrix and additives
- Physical properties: Density 1.1 g/cm<sup>3</sup> (20% lighter than glass fiber equivalents), tensile strength 45-60 MPa, flexural modulus 4-6 GPa meeting automotive interior structural requirements

### **Manufacturing Process and Integration:**

- Compression molding process using pre-consolidated fiber mats with 90-second cycle times achieving production rates of 40 parts per hour per press
- Surface finishing through in-mold coating technologies or secondary covering with textile or synthetic leather maintaining luxury appearance standards
- Full integration with existing production lines requiring minimal capital investment (\$2-3 million per production line) with payback period under 3 years

### **Environmental and Economic Performance Data:**

- Weight reduction: 20-30% lighter than glass fiber composite equivalents, contributing to vehicle lightweighting targets and 2-4% fuel efficiency improvement for affected components
- Carbon footprint reduction: 40% lower lifecycle CO<sub>2</sub> emissions per component (8-12 kg CO<sub>2</sub>-eq per door panel) compared to glass fiber equivalents when including cultivation carbon sequestration benefits
- Cost competitiveness: Achieved price parity with glass fiber composites at \$15-25 per kg finished component through lower material costs offsetting slightly higher fiber preparation expenses
- Recyclability: 95% of component mass recyclable through mechanical grinding and reprocessing or thermal energy recovery, exceeding regulatory requirements and supporting circular economy objectives

Polymer blend systems combining multiple biopolymers exploit synergistic effects where properties of individual polymers complement each other, addressing limitations of single-polymer systems. PLA/PHA blends containing **10-30% PHA** improve toughness and flexibility (elongation at break increasing from 3-6% for pure PLA to 8-15% for blends) while maintaining biodegradability and reducing brittleness issues limiting pure PLA applications (Luengo et al., 2003). PLA/starch blends incorporating 20-40% starch reduce material costs by 25-40% and accelerate biodegradation by providing readily digestible starch component promoting microbial colonization, though requiring careful compatibilization through reactive extrusion or coupling agents to prevent phase separation and maintain mechanical integrity. Nanofiller incorporation including cellulose nanocrystals, nano-clays, or carbon nanotubes at loadings of 1-5% enhances mechanical properties (15-30% strength increases, 20-50% modulus improvements), thermal stability (10-30°C increases in degradation temperatures), and barrier properties (30-60% reductions in oxygen permeability) while maintaining biodegradability when using bio-based nanofillers at modest loading levels.

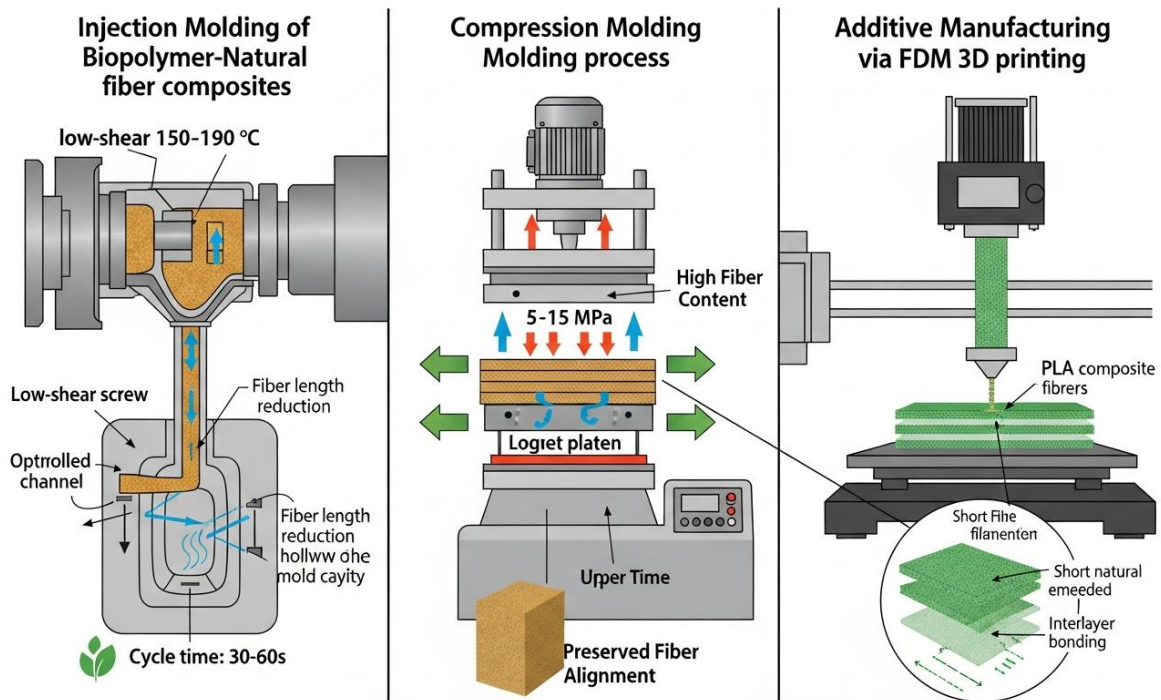
### **5.3 Processing Technologies for Biodegradable Composite Manufacturing**

#### **5.3.1 Injection Molding and Compression Molding Processes**

**Injection molding** represents the dominant manufacturing process for high-volume production of biodegradable composite components, offering cycle times of **30-90 seconds** for typical parts, dimensional tolerances of  $\pm 0.1-0.3\text{mm}$ , and excellent surface finish quality suitable for consumer-facing applications without secondary

finishing. Processing parameters for biodegradable composites require careful optimization to prevent thermal degradation of both natural fibers (decomposition initiating above 200°C) and certain biopolymers (PHA degradation accelerating above 185°C), necessitating temperature profiles of 160-190°C for PLA-based composites and 150-175°C for PHA-based systems, compared to 200-280°C for conventional engineering thermoplastics (Mohanty et al., 2002). Fiber length degradation during injection molding represents a critical challenge, with high shear forces reducing initial fiber lengths from 3-6mm in compounded pellets to 0.3-1.5mm in molded parts, reducing reinforcement efficiency by 40-60% compared to compression-molded equivalents with preserved fiber lengths.

Advanced injection molding techniques address fiber degradation through process modifications including **low-shear screw designs** (compression ratios of 2:1 to 2.5:1 versus 3:1 to 4:1 for conventional screws), reduced screw speeds (50-100 rpm versus 100-200 rpm for standard polymers), and optimized gate designs minimizing flow restrictions and shear stress concentrations. Gas-assist injection molding introducing nitrogen gas at 10-20 MPa during filling reduces required injection pressures by 30-50%, minimizing fiber breakage while creating hollow sections that reduce part weight by 15-30% and material consumption by similar margins without sacrificing structural integrity. Multi-shot injection molding creates hybrid structures combining biodegradable structural cores with conventional polymer outer layers or decorative surfaces, enabling gradual market transition and performance optimization for applications requiring specific surface characteristics (chemical resistance, wear resistance, aesthetics) while maintaining structural sustainability.



**Compression molding** processes natural fiber mat or sheet molding compound (SMC) materials under heat and pressure, achieving superior mechanical properties compared to injection molding through preservation of fiber length and orientation while accommodating higher fiber volume fractions (40-60% versus 20-40% for injection molding). Processing involves heating mold tools to 140-180°C, placing pre-weighed fiber mat or SMC charges, closing molds under pressures of **5-15 MPa**, and maintaining conditions for 2-5 minutes enabling complete matrix flow and consolidation (Faruk et al., 2012). The longer cycle times (3-8 minutes total including part removal and mold preparation) limit compression molding to medium-volume applications (1,000-50,000 parts annually) where superior mechanical performance justifies reduced production rates, particularly for automotive structural panels, furniture components, and construction materials requiring high strength and stiffness.

### 5.3.2 Additive Manufacturing and 3D Printing Technologies

**Fused deposition modeling (FDM)** has emerged as the dominant additive manufacturing technique for biodegradable composites, extruding thermoplastic filaments through heated nozzles (190-220°C for PLA composites) and depositing material layer-by-layer to create complex geometries impossible or uneconomical through conventional manufacturing.

**Table 5.2: Additive Manufacturing Technologies for Biodegradable Composites**

<b>Technology</b>	<b>Build Rate (cm<sup>3</sup>/hour)</b>	<b>Layer Resolution (μm)</b>	<b>Part Strength (% of molded)</b>	<b>Fiber Length Compatible (mm)</b>	<b>Primary Applications</b>
FDM (Standard)	20-50	100-300	40-60	<0.2	Prototypes, low-stress parts, consumer products
FDM (Continuous Fiber)	10-30	150-400	70-90	Continuous	Structural components, tooling, aerospace
Material Jetting	5-15	16-32	50-70	N/A (liquid resin)	High-detail models, dental, jewelry
SLS (Selective Laser Sintering)	15-40	80-150	60-80	0.2-0.8	Functional prototypes, end-use parts, complex geometries
Binder Jetting	100-300	100-200	30-50	0.5-2.0	Large parts, architectural models, sand casting molds

PLA-based filaments dominate commercial availability due to favorable processing characteristics including low warpage, minimal

thermal contraction, and good layer adhesion, with pure PLA achieving mechanical properties in printed parts of **40-60% of injection-molded equivalents** due to interlayer weakness and porosity from incomplete layer fusion (Gkartzou et al., 2017). Natural fiber reinforced PLA filaments incorporating 10-30% wood flour, bamboo, or hemp fibers improve stiffness by 20-40% and create aesthetic effects mimicking natural wood while maintaining printability, though achieving only modest strength improvements (5-15%) due to fiber length limitations (typically <200  $\mu\text{m}$ ) imposed by nozzle diameter constraints.

**Continuous fiber reinforcement** in additive manufacturing represents a breakthrough enabling production of structurally viable parts with mechanical properties approaching conventionally manufactured composites, achieved through co-extrusion systems depositing continuous natural fiber tows (flax, hemp) embedded within thermoplastic matrix achieving fiber volume fractions of 25-40%. These systems produce parts with tensile strengths of **100-180 MPa** and flexural modulus values of 10-20 GPa, representing 70-90% of compression-molded equivalent properties while enabling complex geometries, functional integration, and on-demand production eliminating tooling costs and inventory requirements (Matsuzaki et al., 2016). Applications expand beyond prototyping to include production tooling, custom orthotic devices, aerospace components, and spare parts for legacy equipment where traditional manufacturing economics prove prohibitive for low-volume requirements.

Selective laser sintering (SLS) processes powder bed materials using CO<sub>2</sub> lasers (30-100W power) to selectively fuse particles creating fully dense three-dimensional parts without support structures, enabling

geometric complexity including overhangs, internal channels, and nested assemblies impossible through other techniques. Biodegradable SLS materials include PLA powders achieving part densities of 95-98% and mechanical properties reaching **60-80% of injection-molded references**, with particle size distributions (50-100  $\mu\text{m}$  median diameter) and sphericity critical for powder flow and packing density influencing process reliability and part quality. Natural fiber incorporation in SLS powders faces challenges from fiber aspect ratios disrupting powder flow and laser absorption characteristics varying with fiber content, though successful formulations incorporating 10-20% wood or cellulose fibers achieve modulus improvements of 25-45% while maintaining processability. The higher equipment costs (\$100,000-500,000) and material costs (\$60-100/kg) position SLS for specialized applications including medical devices, customized consumer products, and aerospace components where geometric freedom and performance justify premium pricing.

### **5.3.3 Resin Infusion and Liquid Composite Molding Techniques**

**Vacuum-assisted resin transfer molding (VARTM)** and related liquid composite molding (LCM) processes fabricate high-performance natural fiber composites by placing dry fiber reinforcements in mold cavities and infusing with liquid thermoset or thermoplastic resins under vacuum or positive pressure, enabling production of large, complex parts with excellent surface finish and high fiber volume fractions (50-65%) suitable for structural applications. Bio-based thermoset resins including epoxidized vegetable oils, furan resins, and partially bio-based epoxies (30-50% bio-content) provide matrix options achieving **60-80% of petroleum epoxy mechanical properties** while improving sustainability profiles

and maintaining compatibility with established LCM processing equipment and procedures (Mohanty et al., 2018).

### **Case Study 5.2: Bcomp Natural Fiber Composites in Alpine Ski Manufacturing (Head Skis)**

#### **Background and Industry Context:**

- Partnership initiated in 2018 between Bcomp (Swiss natural fiber composite supplier) and Head (global ski manufacturer) to develop sustainable high-performance skis
- Alpine ski industry faces pressure to reduce environmental footprint while maintaining extreme performance requirements including impact resistance (-20°C to +40°C), fatigue life (>100,000 flexural cycles), and vibration damping
- Traditional ski construction uses carbon fiber, fiberglass, and petroleum-based resins contributing 15-25 kg CO<sub>2</sub>-eq per ski pair production footprint

#### **Technical Implementation and Material Innovation:**

- Bcomp powerRibs™ technology utilizing 3D woven flax fiber reinforcements with controlled fiber orientation achieving specific stiffness matching carbon fiber (40-50 GPa·cm<sup>3</sup>/g)
- Bio-based epoxy resin matrix with 55% bio-content from epoxidized linseed oil maintaining processing compatibility with vacuum infusion systems
- Strategic hybrid design placing flax fibers in vibration-critical zones (ski core and dampening layers) with carbon fiber in high-stress areas (edges, binding mounts)

### **Performance and Manufacturing Data:**

- Mechanical properties: Flexural stiffness 95-105% of all-carbon reference skis, impact resistance exceeding 15 J at -20°C meeting ski safety standards
- Weight: Equivalent or 2-5% lighter than carbon fiber equivalents due to flax density advantage (1.5 g/cm<sup>3</sup> vs 1.8 g/cm<sup>3</sup> for carbon)
- Vibration damping: 30-40% superior damping coefficient compared to carbon fiber skis, improving rider comfort and control through enhanced vibration absorption from natural fiber viscoelastic properties
- Manufacturing integration: Direct substitution in existing vacuum infusion process with no cycle time penalty, requiring only supplier change and minor lay-up procedure modifications

### **Environmental and Market Outcomes:**

- Carbon footprint reduction: 50% reduction in material-related emissions (7-12 kg CO<sub>2</sub>-eq savings per ski pair) through natural fiber cultivation carbon sequestration and bio-resin substitution
- End-of-life: 60% of ski mass potentially compostable or recyclable (excluding metal edges and binding mounts) compared to <20% for conventional construction
- Market reception: Premium positioning maintaining €600-900 retail pricing with "sustainable performance" differentiation, adopted across 15+ ski models by 2023

- Industry influence: Catalyzed natural fiber adoption by competing manufacturers (Rossignol, Fischer) and expansion to other sporting goods (bicycle components, surfboards, paddles)

Reactive thermoplastic resins including caprolactam (nylon-6 precursor) enable in-situ polymerization during infusion creating high-performance thermoplastic composites with superior toughness and recyclability compared to thermoset systems, though requiring precise temperature control (140-180°C) and rapid processing (5-15 minute gel times) demanding sophisticated equipment and process control. PLA-based reactive systems under development promise fully biodegradable LCM processing, though current formulations exhibit limited pot life (15-30 minutes at processing temperatures) and incomplete fiber wet-out requiring continued formulation optimization to achieve commercial viability. The economic competitiveness of LCM processes for biodegradable composites improves for medium-to-large parts (>1 m<sup>2</sup> surface area) produced in low-to-medium volumes (100-10,000 parts annually) where tooling costs (\$10,000-100,000 per mold set) amortize favorably compared to compression molding (\$50,000-500,000) or injection molding (\$100,000-1,000,000) while enabling superior mechanical properties and surface quality.

## **5.4 Applications in Packaging, Automotive and Consumer Engineering**

### **5.4.1 Biodegradable Packaging Solutions: Films, Containers and Protective Materials**

The packaging industry represents the largest market opportunity for biodegradable composites, consuming approximately **146 million tonnes** of plastics annually globally with 40-50% of this volume

comprising single-use applications where biodegradability provides maximum environmental benefit by eliminating persistent waste accumulation (Geyer et al., 2017). PLA films produced through cast or blown film extrusion achieve thicknesses of 20-80  $\mu\text{m}$  with transparency comparable to oriented polypropylene (OPP), oxygen barrier properties of 500-1000  $\text{cm}^3\cdot\mu\text{m}/\text{m}^2\cdot\text{day}\cdot\text{atm}$  suitable for dry food packaging (versus 1500-2000 for OPP and 50-100 for EVOH high-barrier films), and heat seal strengths of 15-25 N/15mm enabling standard packaging equipment operation with minimal modifications. Coating technologies applying nano-cellulose, chitosan, or protein-based layers improve barrier properties by **60-80%**, extending shelf life for moisture-sensitive or oxygen-sensitive products while maintaining compostability.

Rigid packaging including containers, clamshells, and trays produced through injection molding or thermoforming PLA or PLA/starch blends provides sustainable alternatives for food service applications (takeout containers, cutlery, cups) and consumer product packaging (electronics, toys, cosmetics). Performance requirements vary significantly by application, with food contact materials requiring FDA approval demonstrating migration limits <50 ppb for extraction substances and thermal stability preventing deformation during hot-fill operations (85-95°C) or microwave heating (Auras et al., 2004). Modified PLA grades incorporating crystallization promoters or heat-resistant additives achieve heat deflection temperatures of **100-120°C** (versus 55-65°C for standard PLA), enabling applications previously requiring polystyrene or polypropylene while maintaining compostability and achieving price points of \$2.5-3.5/kg competitive with conventional materials when regulatory compliance costs and brand value are considered.

**Protective packaging** applications including loose-fill peanuts, cushioning materials, and molded foam inserts leverage starch-based biodegradable foams produced through extrusion-expansion processes or compression molding of foamed sheets, achieving densities of 15-60 kg/m<sup>3</sup> with compression strengths of 0.05-0.3 MPa and recovery characteristics enabling multiple impact protection. These materials dissolve completely in water (facilitating disposal through standard wastewater systems), compost within 30-90 days under industrial or home composting conditions, and cost \$1.5-2.5/kg representing price parity with expanded polystyrene when waste disposal fees are included. Major e-commerce and electronics companies including Dell, IKEA, and Samsung have adopted starch-based protective packaging across product lines, collectively diverting an estimated **50,000-75,000 tonnes annually** of expanded polystyrene from waste streams while improving packaging sustainability credentials important for corporate environmental goals and consumer preferences.

#### **5.4.2 Automotive Lightweighting and Interior Component Applications**

Automotive applications of biodegradable natural fiber composites focus primarily on interior non-structural components including door panels, seat backs, trunk liners, headliners, and instrument panel substrates where weight reduction contributes to fuel efficiency improvements while biodegradability supports end-of-life vehicle recycling targets mandated by regulations including the EU End-of-Life Vehicle Directive requiring **85% vehicle recyclability** by weight (Faruk et al., 2012). Natural fiber composites achieve 20-30% weight reductions compared to glass fiber equivalents for equivalent stiffness, translating to 2-4% overall vehicle weight reduction when

applied comprehensively across interior components, contributing to fuel economy improvements of 0.3-0.6 L/100km and CO<sub>2</sub> emission reductions of 7-15 g/km over vehicle lifecycle.

### **Case Study 5.3: Ford Motor Company Soy-Based Foam and Composite Interior Components**

#### **Background and Sustainability Strategy:**

- Initiated in 2007 as part of comprehensive sustainable materials program targeting 25% bio-based material content in vehicle interiors by 2025
- Addressed petroleum dependency in polyurethane foams (100 million pounds annually in Ford vehicles), interior plastics, and composite components
- Aligned with corporate commitments to reduce manufacturing CO<sub>2</sub> emissions by 30% per vehicle and water consumption by 72% between 2010-2025

#### **Material Development and Technical Specifications:**

- Soy-based polyurethane foam replacing petroleum polyol with soy oil polyol at 5-40% replacement levels depending on application (seat cushions, head restraints, armrests)
- Mechanical performance: Compression strength and resilience within 5% of petroleum-based equivalents, meeting automotive interior durability standards including 100,000 cycle fatigue testing
- Natural fiber composites (kenaf, cellulose, wheat straw) replacing 50-70% glass fiber in door panel substrates, package trays, and floor consoles

### **Manufacturing Scale and Implementation:**

- Deployed across 60+ vehicle models globally including F-150, Mustang Mach-E, Explorer, and Escape platforms
- Annual consumption: 18 million pounds soy-based foam (approximately 25,000 tonnes) in North American production
- Supply chain: Partnerships with 15+ tier-1 and tier-2 suppliers ensuring material availability and quality consistency across production facilities

### **Economic and Environmental Performance:**

- Cost neutral to 3-5% premium compared to conventional materials, offset by weight savings reducing shipping costs and improving fuel economy
- Lifecycle emissions reduction: 15-20% lower CO<sub>2</sub> footprint for soy foam (0.5-1.0 kg CO<sub>2</sub>-eq savings per vehicle) and 30-40% for natural fiber composites (2-4 kg CO<sub>2</sub>-eq savings per vehicle)
- End-of-life: Improved recyclability with 80-90% of natural fiber components recoverable through mechanical recycling or thermal energy recovery
- Industry leadership: Established Ford as automotive sustainability leader, influencing adoption by Toyota, BMW, and Volkswagen Group

Manufacturing process integration represents a critical success factor, with automotive suppliers investing \$5-15 million per production line to establish compression molding, injection molding, or thermoforming capabilities specifically configured for natural fiber composites including fiber preparation equipment, modified tooling accommodating longer cycle times (30-50% increases), and quality

control systems monitoring fiber distribution and surface quality. The business case strengthens as volumes increase and learning curves reduce scrap rates from initial 8-12% to optimized 3-5%, while regulatory compliance becomes increasingly stringent with initiatives including California's Cleaner Cars and Cleaner Trucks regulations incentivizing zero-emission vehicles where every kilogram of weight reduction improves electric range by approximately 0.1-0.15 kilometers.

Acoustic performance represents an unexpected benefit of natural fiber composites, with sound absorption coefficients of **0.6-0.9** at mid-frequencies (500-2000 Hz) compared to 0.3-0.5 for glass fiber composites, enabling noise reduction of 3-6 dB in vehicle interiors through door panel and headliner applications improving perceived quality and passenger comfort (Sanjay et al., 2018). The micro-porous structure of natural fibers combined with inherent damping properties creates superior acoustic absorption without additional damping treatments, providing 15-25% cost savings in acoustic package engineering while reducing weight and improving sustainability metrics. Future developments target semi-structural applications including seat frames, cross-car beams, and floor pan reinforcements requiring ultimate tensile strengths exceeding 150 MPa and impact energy absorption >50 J, achievable through hybrid formulations and advanced fiber architectures currently under development.

#### **5.4.3 Consumer Products and Biomedical Device Applications**

Consumer electronics and appliance housings represent growing applications for biodegradable composites as manufacturers respond to regulatory pressures (WEEE Directive addressing electronic waste),

corporate sustainability commitments (Apple, Dell, HP targeting carbon neutrality), and consumer preferences for environmentally responsible products. PLA and PLA-composite injection molded housings provide suitable properties for low-stress applications including computer peripherals (keyboards, mice), small appliances (coffee makers, toasters), and power tool housings, achieving impact strengths of **15-35 kJ/m<sup>2</sup>** (versus 50-100 kJ/m<sup>2</sup> for ABS) sufficient for consumer applications with careful design including increased wall thicknesses (3-4mm versus 2-3mm for ABS) and reinforcement ribs at stress concentrations (Jamshidian et al., 2010). Surface finish quality, dimensional stability, and colorability match conventional plastics enabling direct substitution with minimal aesthetic compromise, though thermal limitations restrict applications to components experiencing <60°C service temperatures.

**Biomedical applications** exploit biodegradability as a functional advantage, with PLA and PLA-composite implants, surgical devices, and drug delivery systems degrading in vivo through hydrolytic and enzymatic mechanisms eliminating secondary removal surgeries, reducing patient trauma, and lowering healthcare costs. Orthopedic fixation devices including screws, pins, and plates manufactured from PLA or PLA/hydroxyapatite composites provide initial mechanical support (tensile strength 50-70 MPa) during bone healing (6-12 weeks) then gradually degrade through hydrolysis over 12-24 months as healed bone tissue reestablishes structural integrity (Luengo et al., 2003). The degradation rate tuning through polymer molecular weight selection (higher molecular weights slowing degradation), copolymerization (PLA-PGA blends accelerating degradation), or composite formulation (calcium phosphate fillers buffering acidic degradation products) enables matching implant

degradation timeline to tissue regeneration kinetics optimizing clinical outcomes.

Tissue engineering scaffolds fabricated through additive manufacturing or electrospinning create three-dimensional porous structures (porosity 70-90%, pore sizes 100-500  $\mu\text{m}$ ) supporting cell infiltration, proliferation, and differentiation while gradually degrading as newly formed tissue replaces scaffold material. PLA-based scaffolds demonstrate biocompatibility supporting attachment and growth of multiple cell types (osteoblasts, chondrocytes, fibroblasts) with degradation products (lactic acid) metabolized through normal biochemical pathways eliminating toxicity concerns present with non-degradable implant materials. Commercial success examples include Ethicon's Vicryl sutures (PLA-PGA copolymer, \$250 million annual sales), Biomet's Bio-Interference screws (PLA orthopedic fixation, \$50 million annual sales), and numerous drug delivery devices providing controlled release of therapeutics over weeks to months through polymer erosion-mediated release mechanisms creating \$2-3 billion annual market for biodegradable medical polymers.

## **5.5 Summary**

Biodegradable composite materials have matured from niche research concepts to commercially viable engineering materials supporting diverse applications across packaging, automotive, consumer products, and biomedical sectors, offering mechanical properties competitive with conventional materials while providing 30-70% reductions in lifecycle carbon emissions and complete end-of-life biodegradability. Biopolymer matrices including PLA (tensile strength 50-70 MPa, modulus 3-4 GPa) and PHA (complete marine

biodegradation within 60-90 days) combined with natural fiber reinforcements (flax, hemp, kenaf achieving specific strength 350-650 MPa·cm<sup>3</sup>/g) create sustainable composites achieving 60-90% of glass fiber composite properties at equivalent or lower costs when environmental externalities are internalized. Advanced processing technologies including injection molding (30-90 second cycles), compression molding (superior mechanical properties through fiber length preservation), and additive manufacturing (enabling geometric complexity and customization) support commercial production across volume scales from prototype to mass production.

Market adoption accelerates through converging regulatory pressures (single-use plastic bans, vehicle recyclability mandates), corporate sustainability commitments, and improving cost competitiveness (achieving price parity at \$2.5-3.5/kg for many applications), with global biodegradable plastics market reaching \$19.8 billion by 2027 growing at 14.3% annually. Successful implementations including Mercedes-Benz natural fiber interior components (40% natural fiber content in 50+ models), Ford soy-based foams (18 million pounds annually), and diverse packaging applications (50,000-75,000 tonnes starch-based protective packaging) demonstrate technical viability and economic competitiveness while quantifying environmental benefits including weight reductions of 20-30%, emission reductions of 30-50%, and improved recyclability supporting circular economy objectives aligned with SDG 12 and SDG 13.

## References

- [1] Auras, R., Harte, B., & Selke, S. (2004). An overview of polylactides as packaging materials. *Macromolecular Bioscience*, 4(9), 835-864. <https://doi.org/10.1002/mabi.200400043>

- [2] Avérous, L. (2004). Biodegradable multiphase systems based on plasticized starch: A review. *Journal of Macromolecular Science, Part C: Polymer Reviews*, 44(3), 231-274. <https://doi.org/10.1081/MC-200029326>
- [3] Faruk, O., Bledzki, A. K., Fink, H. P., & Sain, M. (2012). Biocomposites reinforced with natural fibers: 2000–2010. *Progress in Polymer Science*, 37(11), 1552-1596. <https://doi.org/10.1016/j.progpolymsci.2012.04.003>
- [4] Geyer, R., Jambeck, J. R., & Law, K. L. (2017). Production, use, and fate of all plastics ever made. *Science Advances*, 3(7), e1700782. <https://doi.org/10.1126/sciadv.1700782>
- [5] Gkartzou, E., Koumoulos, E. P., & Charitidis, C. A. (2017). Production and 3D printing processing of bio-based thermoplastic filament. *Manufacturing Review*, 4, 1-14. <https://doi.org/10.1051/mfreview/2016020>
- [6] Grand View Research. (2020). *Biodegradable plastics market size, share & trends analysis report*. San Francisco: Grand View Research, Inc.
- [7] Jamshidian, M., Tehrany, E. A., Imran, M., Jacquot, M., & Desobry, S. (2010). Poly-lactic acid: Production, applications, nanocomposites, and release studies. *Comprehensive Reviews in Food Science and Food Safety*, 9(5), 552-571. <https://doi.org/10.1111/j.1541-4337.2010.00126.x>
- [8] Luengo, J. M., García, B., Sandoval, A., Naharro, G., & Olivera, E. R. (2003). Bioplastics from microorganisms. *Current Opinion in Microbiology*, 6(3), 251-260. [https://doi.org/10.1016/S1369-5274\(03\)00040-7](https://doi.org/10.1016/S1369-5274(03)00040-7)
- [9] Matsuzaki, R., Ueda, M., Namiki, M., Jeong, T. K., Asahara, H., Horiguchi, K., ... & Todoroki, A. (2016). Three-dimensional printing of continuous-fiber composites by in-nozzle impregnation. *Scientific Reports*, 6, 23058. <https://doi.org/10.1038/srep23058>
- [10] Mohanty, A. K., Misra, M., & Hinrichsen, G. (2000). Biofibres, biodegradable polymers and biocomposites: An overview. *Macromolecular Materials and Engineering*, 276-277(1), 1-24.

[https://doi.org/10.1002/\(SICI\)1439-2054\(20000301\)276:1<1::AID-MAME1>3.0.CO;2-W](https://doi.org/10.1002/(SICI)1439-2054(20000301)276:1<1::AID-MAME1>3.0.CO;2-W)

- [11] Mohanty, A. K., Vivekanandhan, S., Pin, J. M., & Misra, M. (2018). Composites from renewable and sustainable resources: Challenges and innovations. *Science*, 362(6414), 536-542. <https://doi.org/10.1126/science.aat9072>
- [12] Pickering, K. L., Efendy, M. G. A., & Le, T. M. (2016). A review of recent developments in natural fibre composites and their mechanical performance. *Composites Part A: Applied Science and Manufacturing*, 83, 98-112. <https://doi.org/10.1016/j.compositesa.2015.08.038>
- [13] Sanjay, M. R., Madhu, P., Jawaid, M., Senthamaraikannan, P., Senthil, S., & Pradeep, S. (2018). Characterization and properties of natural fiber polymer composites: A comprehensive review. *Journal of Cleaner Production*, 172, 566-581. <https://doi.org/10.1016/j.jclepro.2017.10.101>



# Interdisciplinary Scientific and Technical Research for SDG Achievement

December 2025



**Dr. M. Kotteeswaran** is currently an Associate Professor and Research Supervisor in the School of Management Studies at Vels Institute of Science, Technology and Advanced Studies, Chennai. He guides eight Ph.D. scholars, of whom two have submitted their theses, and serves as Board of Studies Member in leading engineering institutions in Tamil Nadu. With 24 years of academic experience, he has published 15 Scopus papers, 40 UGC CARE articles, authored six textbooks and obtained six national and international patents. He is Editor-in-Chief of an international journal and has received major awards. He also served as External Examiner and visited universities in Malaysia.



**Dr. J. Sathiya Savithri** is currently working as the Head and Assistant Professor in the PG and Research Department of Chemistry at Theivanai Ammal College for Women (Autonomous), Villupuram. She holds a Ph.D. in Organic Chemistry from the University of Madras and received the prestigious Thiru R. H. Ramachandra Rao Gold Medal. Her research expertise spans dendrimer chemistry, photophysical studies, and phytochemical analysis, with 19 publications in reputed international journals. She has guided numerous UG and PG students and actively contributes to conferences, seminars, and academic committees. Her strong leadership, research productivity, and academic service reflect her dedication to advancing chemical sciences.



**Dr. Absara FDO S, M.Sc., M.Phil., Ph.D.** serves as an Assistant Professor in the department of Chemistry (School of Basic Sciences), Vels Institute of Science, Technology and Advanced Studies (VISTAS), Chennai. She earned her doctoral degree in Chemistry from University of Madras in 2024. She has expertise in the fields of Electrochemistry, nano chemistry, bioinorganic Chemistry and Environmental Chemistry. She has a teaching experience of 12 years in various academic institutions. She has received the research Excellence award for her research proficiency. She has guided B.Sc. and M.Sc. projects in Chemistry. She has a passion for innovative research and inspiring teaching.



**Dr. M. Ramamurthy** is working as Assistant Professor in the department of Mechanical engineering, Academy of Maritime Education and Training (AMET), Deemed to be University, Chennai. He completed the Ph.D degree in 2023 at Anna University, Chennai. His Research area is Friction Stir Welding. He got his Master's degree in Manufacturing Engineering in the year 2011 from Anna University, Trichy. He obtained Bachelor's degree in Mechanical engineering from Bharathidasan University during the year 1997. He had around 8 years industry experience and 17 years Academic experience. He had published 7 technical articles in Scopus indexed journals, and three patents.

## SCIENTIFIC RESEARCH REPORTS

(A Book Publisher, approved by Govt. of India)

I Floor, S S Nagar, Chennai - 600 087,  
Tamil Nadu, India.

[editors@srrbooks.in](mailto:editors@srrbooks.in), [contact@srrbooks.in](mailto:contact@srrbooks.in)

[www.srrbooks.in](http://www.srrbooks.in)

ISBN 978-819934028-2



9 788199 340282